

# Identifying Higgsino-like neutralino with a keV-scale dark matter

---

**Juhi Dutta, Biswarup Mukhopadhyaya and Santosh Kumar Rai**

*Regional Centre for Accelerator-based Particle Physics,  
Harish-Chandra Research Institute, HBNI,  
Chhatnag Road, Jhusi, Allahabad 211019, India*

*E-mail:* [juhidutta@hri.res.in](mailto:juhidutta@hri.res.in), [biswarup@hri.res.in](mailto:biswarup@hri.res.in),  
[skrai@hri.res.in](mailto:skrai@hri.res.in)

**ABSTRACT:** The presence of a Higgsino-like neutralino NLSP and a keV scale gravitino ( $\tilde{G}$ ) LSP opens up new decay modes of the NLSP, mainly to a Higgs/ $Z$  boson and the LSP. Besides, a keV-scale gravitino as a warm dark matter candidate salvages a relatively-light Higgsino-like NLSP from dark matter constraints. We focus on the prospects of observing  $\geq 1b + \ell^+\ell^- + \cancel{E}_T$  signal at the LHC. A distinguishing feature of this scenario is the production of longitudinal  $Z$  bosons in neutralino decays, unlike in the case of gaugino-like neutralinos, where the  $Z$  is mostly transverse. The polarisation information of the parent  $Z$  boson gets reflected in the angular distributions of the decay leptons and in some other variables derived therefrom.

**KEYWORDS:** Supersymmetry Phenomenology, Large Hadron Collider, Higgsino-like NLSP, Longitudinal  $Z$  boson

---

## Contents

<b>1</b>	<b>Introduction</b>	<b>1</b>
<b>2</b>	<b>Higgsino-dominated NLSP with keV LSP</b>	<b>4</b>
<b>3</b>	<b>Higgsino NLSP decays</b>	<b>5</b>
<b>4</b>	<b>Existing LHC limits</b>	<b>10</b>
<b>5</b>	<b>Benchmarks for our analysis</b>	<b>11</b>
<b>6</b>	<b>LHC Signals</b>	<b>13</b>
<b>7</b>	<b>A Distinguishing Feature: Longitudinal vs Transverse Gauge bosons</b>	<b>22</b>
<b>8</b>	<b>Summary and Conclusions</b>	<b>29</b>

---

## 1 Introduction

In the light of the 13 TeV LHC Run 2 results [1, 2], both experimentalists and theorists are leaving no stone unturned to interpret results of different supersymmetric (SUSY) scenarios, primarily to ensure no glaring gaps are left in the current search strategies such that the signals may slip through them. Although bounds on sparticle masses from LHC are steadily increasing, they are derived in the context of simplified scenarios. However, generic features on collider signals are helpful to investigate, if such features reflect the spectrum and the composition of the superparticle states.

The  $R$ -parity conserving minimal supersymmetric standard model (MSSM) ensures a stable, neutral, colourless dark matter candidate, generally the lightest neutralino ( $\tilde{\chi}_1^0$ ) which is the lightest SUSY particle (LSP). Depending on its composition, it could be either a democratic admixture of gaugino and higgsino states or dominantly bino-like, wino-like or higgsino-like. The DM composition faces stringent constraints from direct detection cross-sections as well as from relic density measurements by Planck [3]. For example, a bino-dominated  $\tilde{\chi}_1^0$  with an appropriate small admixture of higgsinos can by and large be consistent with relic density as well as direct search constraints, while for a wino-like LSP, the annihilation cross-section would be large owing to the SU(2) gauge couplings, and it is thus strongly constrained

by direct search data, unless its mass is  $\geq 2 \text{ TeV}$ <sup>1</sup>. A light higgsino-like LSP is disfavoured from direct dark matter searches [5, 6]. Conversely, the relic density being inversely proportional to the annihilation cross-section, shows an underabundance for wino or higgsino-like LSP whereas a bino-like LSP can lead to an overabundance unless co-annihilation occurs at an adequate rate. Mixed bino-higgsino or bino-wino dark matter scenarios could be more consistent from these standpoints [7]. The presence of a lighter particle such as a gravitino or an axino as the lightest SUSY particle relaxes these constraints on the composition of the lightest neutralino  $\tilde{\chi}_1^0$ , which now serves as the next-to-lightest sparticle (NLSP). Gravitinos are the LSP in models like gauge mediated supersymmetry breaking with low scale of SUSY breaking. Here, the gravitino mass scale maybe lighter than the MSSM sparticle masses if the scale of SUSY breaking is light enough to allow a light gravitino mass governed by [8–10]:

$$m_{\tilde{G}} = \frac{\langle F \rangle}{\sqrt{3}M_{Pl}} \quad (1.1.1)$$

where  $m_{\tilde{G}}$  is the mass of the gravitino,  $\langle F \rangle$  is the SUSY breaking scale and  $M_{Pl}$  is the Planck scale. This means that depending on the SUSY breaking scale  $\langle F \rangle$ , the gravitino can be as light as  $\mathcal{O}(\text{keV})$ . A light gravitino with mass of few keV is motivated to be a warm dark matter candidate [11–13]. In this work we consider the LHC signals of a higgsino-dominated NLSP where one has such a light gravitino LSP. Our study would also apply to scenarios where an axino is the dark matter candidate.

Signals for a dominantly higgsino-like  $\tilde{\chi}_1^0$  NLSP with a gravitino LSP has been studied by experimental collaborations at the LHC. A primarily higgsino-like  $\tilde{\chi}_1^0$  NLSP is found to decay dominantly to either the Higgs or  $Z$  boson along with gravitino. Since the light standard model (SM) like Higgs has the largest decay probability to  $b\bar{b}$ , this leads to a final state dominated by hard  $b$ -tagged jets along with large missing transverse momentum (MET)  $\cancel{E}_T$  and additional light jets/leptons arising from accompanying  $Z$  boson. Signatures for the higgsino-like NLSP's have been studied in the context of Tevatron [14, 15] and also at LHC where both CMS [16] and ATLAS [17] have looked at multiple  $b$ -jets + MET, dilepton and multilepton states to constrain a higgsino-like NLSP scenario.

In this work, we aim to study signatures of a low-lying higgsino sector in the presence of a light gravitino LSP with emphasis on determining how the NLSP nature can be convincingly identified. To do this one would like to reconstruct the decay products of the NLSP. As the higgsino NLSP would decay to a light Higgs or a  $Z$  boson, we may be able to observe their properties by appropriately reconstructing the Higgs through the  $b$ -jets arising from its decay as well as the  $Z$  boson through the opposite sign dilepton pair from the gauge boson's decay respectively. We note here

---

<sup>1</sup>In addition a bino-wino mixed  $\tilde{\chi}_1^0$  would also satisfy the relic density but direct searches stringently constrain these scenarios to heavy masses [4].

a very important and interesting feature of the decay of the NLSP. It is expected that the  $Z$  boson arising from the higgsino-like  $\tilde{\chi}_1^0$  decay would be dominantly *longitudinal* (Goldstone boson), primarily following the *equivalence theorem* where, after electroweak symmetry breaking the neutral Goldstone boson constitutes the longitudinal mode of the  $Z$  boson responsible for its mass. This property if observed in the decay of the NLSP would exclusively point towards the presence of a higgsino-like  $\tilde{\chi}_1^0$ , helping us identify the nature of the NLSP. The direct production of the electroweak neutralino NLSP would be limited at the LHC as their mass becomes larger. However, the property of the NLSP could still be studied if they are produced in cascade decays of strongly interacting sparticles. We therefore study the effect of including the strong sector in exploring the compositions of the NLSP as well as from the direct production of the low-lying electroweakinos (still allowed by experiments) and propose some new kinematic variables which help identify the NLSP. Thus, the salient points of our study are as follows:

- We consider a naturally compressed low-lying higgsino sector as well as partially and/or fully compressed spectra with the strongly interacting sparticles sitting above the NLSP. The sparticles decay via cascades to the NLSP which further decays to a Higgs and a  $Z$  boson thereby giving rise to at least 1  $b$ -jet and opposite-sign same flavour dileptons along with missing transverse energy in the final state.
- The characteristic features of a longitudinal  $Z$  boson arising from decay of the higgsino-like  $\tilde{\chi}_1^0$  are studied by utilising angular variables of the negatively charged lepton. In order to distinguish it from transversely polarised  $Z$  bosons coming from other sources, we compare our results with the complementary admixture of NLSP, especially gaugino-dominated neutralinos as well as the SM background.
- We observe that for a spectrum with a heavy NLSP, reflecting overall compression with respect to the strong sector leads to an increased fraction of the longitudinal mode in the  $Z$  boson arising from the NLSP decay.
- New variables enhancing the asymmetry in the angular distributions of the negatively charged lepton have been proposed in order to characterize a longitudinally polarized  $Z$  boson in comparison to a transversely polarized  $Z$  boson. Such asymmetry variables distinctly vary depending on the higgsino-gaugino admixture of the NLSP and crucially capture the effect of the equivalence theorem for a heavy NLSP in a somewhat compressed spectrum.

The paper is organised as follows. In section 2 we discuss the current scenario with the higgsino NLSP and gravitino LSP followed by the decay properties of the higgsinos in section 3. In section 4, we discuss the experimental status of a higgsino-like NLSP

with a light gravitino LSP at LHC. In section 5, we choose some benchmarks to study the available parameter space. We perform the collider study and discuss our results at the high luminosity run of LHC in section 6. In section 7, we distinguish between the features of longitudinal and transverse gauge bosons. Section 8 summarises the main conclusions of our work.

## 2 Higgsino-dominated NLSP with keV LSP

In our work, we discuss light higgsino-like NLSP as a possible consequence of general phenomenological MSSM. Since no hint of SUSY has yet shown up at direct searches, various possible configurations of the lightest neutralino,  $\tilde{\chi}_1^0$ , leading to distinct signals at colliders are of interest. Such a light higgsino-like  $\tilde{\chi}_1^0$  is characterized by a light  $\mu$  parameter and heavy bino, wino soft mass parameters, i.e,  $|\mu| \ll M_1, M_2$ . Besides, low  $\mu$  parameter is also a preferred choice from naturalness perspective [18–23]. However  $\tilde{\chi}_1^0$  may not be the LSP in many situations. In such cases there can be several other candidates for LSP such as gravitinos, axinos, sneutrinos etc.

The gravitino is the spin 3/2 superpartner of the spin 2 graviton in local SUSY. Upon spontaneous SUSY breaking, there arises a massless Weyl fermion known as the goldstino ( $\tilde{G}$ ), owing to the breaking of the fermionic generators of SUSY. After electroweak symmetry breaking, the gravitino acquires mass by absorbing the goldstino which form the spin 1/2 components of the massive gravitino.

It is in fact the goldstino (which constitutes the longitudinal part of the gravitino) that is produced in processes at energy scales much higher than the gravitino mass. For a light gravitino, a TeV-scale sparticle then decays to an SM particle and the goldstino with a coupling enhanced by a factor of  $(M_{Pl}m_{\tilde{G}})^{-1}$  and hence may decay within the collider [24]. Hence, it is the goldstino mode of the gravitino that is important for collider phenomenology. The goldstino ( $\tilde{G}$ ) Lagrangian is [8]:

$$\mathcal{L}_{goldstino} = i\tilde{G}^\dagger \bar{\sigma}^\mu \partial_\mu \tilde{G} - \frac{1}{\langle F \rangle} \tilde{G} \partial_\mu j^\mu + c.c \quad (2.2.1)$$

where  $\langle F \rangle$  refers to the *vev* obtained by the SUSY breaking auxiliary field  $F$  and  $j^\mu$  refers to the current involving all other sparticles and SM particles. The couplings of the gravitino to fermion-sfermion, gauge boson-gauginos are computed in Ref. [24].

We now discuss the couplings and decays of a higgsino-like  $\tilde{\chi}_1^0$  NLSP in the presence of a gravitino ( $\tilde{G}$ )<sup>2</sup> LSP before moving on to a numerical analysis in section 3. In addition, we briefly discuss the parameter space region where higgsinos could give rise to a prompt decay. Non-prompt searches (such as searches for charged tracks [25, 26]) for higgsinos would be relevant for  $\tilde{\chi}_1^\pm$  NLSP.<sup>3</sup>

<sup>2</sup>We use  $\tilde{G}$  for the gravitino in the remaining part of the manuscript.

<sup>3</sup>Searches for displaced jets and leptons could be relevant for neutral higgsinos:  $\tilde{\chi}_2^0, \tilde{\chi}_1^0$  in the presence of non-standard LSP candidates [13, 27].

Such a scenario is phenomenologically analogous to a scenario with axino LSP. However since axino couplings to MSSM particles differ from gravitino couplings, similar signals may arise for axino LSP depending on the NLSP masses. For similar mass values of an axino and gravitino, the NLSP decay width is much smaller for an axino LSP which may lead to a long lived NLSP signature, for e.g, charged tracks for  $\tilde{\chi}_1^\pm$  in the colliders [13].

### 3 Higgsino NLSP decays

A higgsino-like  $\tilde{\chi}_1^0$  is characterised by a large higgsino fraction with suppressed gaugino and bino fractions i.e,  $\mu < M_1, M_2$ . In the presence of a light  $\tilde{G}$  LSP, the higgsino-like  $\tilde{\chi}_1^0$  NLSP decays to either a Higgs ( $h$ ) or a  $Z$  boson and  $\tilde{G}$ .<sup>4</sup> Absence of a large bino component leads to a rather suppressed photon mode unless there is substantial gaugino-bino-higgsino admixture [15]. However the photon mode may dominate in case of very light higgsinos where the decay to the Higgs or  $Z$  boson is phase space suppressed. As the coupling of a gravitino to other particles are inversely proportional to its mass( $m_{\tilde{G}}$ ), a lighter gravitino has stronger couplings as compared to a heavier one. The decay width is proportional to  $m_{\tilde{X}}^5$ , where  $m_{\tilde{X}}$  is the mass of the parent sparticle. Hence for a fixed gravitino mass and increasing NLSP mass, the decay width increases and leads to prompt decays. For any sparticle  $\tilde{X}$ , its two-body decay to  $X$  and a gravitino is given as:

$$\Gamma(\tilde{X} \rightarrow X\tilde{G}) = \frac{m_{\tilde{\chi}_1^0}^5}{48\pi M_P^2 m_{\tilde{G}}^2} \left(1 - \frac{m_X^2}{m_{\tilde{X}}^2}\right)^4 \quad (3.3.1)$$

where  $m_X$  refer to the mass of the SM partner of  $\tilde{X}$ . As we are interested in the decay of the neutralino NLSP to the gravitino, the composition of the lightest neutralino becomes an essential characteristic as it would determine what the NLSP finally decays to. The neutralino mass matrix in the basis  $(\tilde{B}, \tilde{W}_3, \tilde{H}_d^0, \tilde{H}_u^0)$  is as follows:

$$M^n = \begin{pmatrix} M_1 & 0 & -M_Z s_W c_\beta & M_Z s_W s_\beta \\ 0 & M_2 & M_Z c_W c_\beta & -M_Z c_W s_\beta \\ -M_Z s_W c_\beta & M_Z c_W c_\beta & 0 & -\mu \\ M_Z s_W s_\beta & -M_Z c_W s_\beta & -\mu & 0 \end{pmatrix}. \quad (3.3.2)$$

Here,  $s_W = \sin \theta_W$ ,  $c_W = \cos \theta_W$  where  $\theta_W$  is the weak mixing angle whereas  $s_\beta = \sin \beta$ ,  $c_\beta = \cos \beta$  where  $\tan \beta = \frac{v_u}{v_d}$  refers to the ratio of the  $vev$ 's of the up-type Higgs doublet ( $H_u$ ) and down-type Higgs doublet  $H_d$ .  $M_Z$  and  $M_W$  are the masses of the  $W$  and  $Z$  boson and  $M_1, M_2$  are the bino and wino soft mass parameters respectively,

---

<sup>4</sup>In presence of  $M_A < \mu$ , the NLSP may also decay into the heavy Higgses [28]. In this study, for simplicity the heavy Higgs masses are kept above the spectrum of interest.

while  $\mu$  is the higgsino mass parameter. Diagonalising the symmetric mass matrix using a unitary matrix  $N$  lead to the neutralino mass eigenstates  $\tilde{\chi}_i^0$  ( $i = 1, \dots, 4$ ).

$$NM^n N^T = \text{diag}(m_{\tilde{\chi}_1^0}, m_{\tilde{\chi}_2^0}, m_{\tilde{\chi}_3^0}, m_{\tilde{\chi}_4^0}) \quad (3.3.3)$$

where  $m_{\tilde{\chi}_1^0} < m_{\tilde{\chi}_2^0} < m_{\tilde{\chi}_3^0} < m_{\tilde{\chi}_4^0}$ .

The chargino mass matrix  $M^c$  in the basis  $(\tilde{W}^+, \tilde{H}_u^+)$  is as follows:

$$M^c = \begin{pmatrix} M_2 & \sqrt{2}M_W s_\beta \\ \sqrt{2}M_W c_\beta & \mu \end{pmatrix}. \quad (3.3.4)$$

Since,  $M^c$  is not a symmetric matrix, we need two unitary matrices  $U$  and  $V$  to diagonalize the matrix. Hence,

$$U^* M^c V^{-1} = \text{diag}(m_{\tilde{\chi}_1^\pm}^2, m_{\tilde{\chi}_2^\pm}^2) \quad (3.3.5)$$

where  $m_{\tilde{\chi}_1^\pm}^2 < m_{\tilde{\chi}_2^\pm}^2$ . Thus, in the limit where  $\mu \ll M_1, M_2$ , ie. the lightest neutralino is dominantly higgsino-like with small gaugino fractions, there are two nearly degenerate higgsino-like neutralinos  $\tilde{\chi}_1^0, \tilde{\chi}_2^0$  and higgsino-like chargino,  $\tilde{\chi}_1^\pm$ . Thus, a low-lying higgsino mass parameter leads to a naturally compressed spectra consisting of three closely lying particles  $\tilde{\chi}_1^0, \tilde{\chi}_2^0$  and  $\tilde{\chi}_1^\pm$ . The mass eigenvalues for the higgsinos at the tree-level are [29, 30]:

$$\begin{aligned} m_{\tilde{\chi}_1^\pm} &= |\mu| \left( 1 - \frac{M_W^2 \sin 2\beta}{\mu M_2} \right) + \mathcal{O}(M_2^{-2}) \\ m_{\tilde{\chi}_{1,2}^0} &= \pm \mu - \frac{M_Z^2}{2} (1 \pm \sin 2\beta) \left( \frac{\sin \theta_W^2}{M_1} + \frac{\cos \theta_W^2}{M_2} \right) \end{aligned} \quad (3.3.6)$$

In the MSSM, the  $\tilde{\chi}_1^0$  is primarily the LSP with different mass hierarchies amongst the higgsinos. Owing to the natural compression in mass amongst the higgsinos,  $\tilde{\chi}_2^0$  and  $\tilde{\chi}_1^\pm$  primarily decay via off-shell gauge bosons ( $W^\pm, Z$ ) to the LSP.  $\tilde{\chi}_2^0$  may also decay via a photon to the LSP at one-loop level. In cases, where  $\tilde{\chi}_2^0$  is the heaviest amongst all the higgsinos, the following are the relevant decay modes of the higgsinos:

$$\begin{aligned} \tilde{\chi}_2^0 &\rightarrow f \bar{f} \tilde{\chi}_1^0, f \bar{f}' \tilde{\chi}_1^\pm, \gamma \tilde{\chi}_1^0 \\ \tilde{\chi}_1^\pm &\rightarrow f \bar{f}' \tilde{\chi}_1^0 \end{aligned} \quad (3.3.7)$$

where  $f$  and  $f'$  are SM fermions. There may be regions in the parameter space where  $\tilde{\chi}_1^\pm$  is heavier than  $\tilde{\chi}_2^0$ , the decays of the  $\tilde{\chi}_2^0$  and  $\tilde{\chi}_1^\pm$  are modified as follows:

$$\begin{aligned} \tilde{\chi}_1^\pm &\rightarrow f \bar{f}' \tilde{\chi}_1^0, f \bar{f}' \tilde{\chi}_2^0 \\ \tilde{\chi}_2^0 &\rightarrow f \bar{f} \tilde{\chi}_1^0, \gamma \tilde{\chi}_1^0 \end{aligned} \quad (3.3.8)$$

In some regions of the parameter space,  $\tilde{\chi}_1^\pm$  may become the lightest of all the higgsinos [29], thereby opening up the following are the decay modes of  $\tilde{\chi}_1^0, \tilde{\chi}_2^0$ :

$$\begin{aligned}\tilde{\chi}_2^0 &\rightarrow f\bar{f}\tilde{\chi}_1^0, f\bar{f}'\tilde{\chi}_1^\pm, \gamma\tilde{\chi}_1^0 \\ \tilde{\chi}_1^0 &\rightarrow f\bar{f}\tilde{\chi}_1^\pm\end{aligned}\tag{3.3.9}$$

However with the charged state being the lightest an alternative light LSP candidate is preferred, which in our case happens to be the gravitino. In the presence of  $\tilde{G}$  LSP, new decay modes open up for the higgsinos. The presence of a non-zero higgsino fraction in  $\tilde{\chi}_1^0$  and  $\tilde{h} - h - \tilde{G}$  vertex ensures the presence of a Higgs boson arising from the decay of  $\tilde{\chi}_1^0$  to a Higgs and  $\tilde{G}$ . Suppressed gaugino fractions imply reduced decay to photons or  $Z$  along with the gravitino which would otherwise proliferate for bino/wino dominated NLSP. However there is substantial branching fraction of  $\tilde{\chi}_1^0$  into  $Z$  and  $\tilde{G}$  in the case of a higgsino-like NLSP as well [14, 15]. This is because after electroweak symmetry breaking, the Goldstone boson forms the longitudinal component of the  $Z$  boson. Similarly,  $\tilde{\chi}_1^\pm$  may also decay to a longitudinal  $W$  along with the  $\tilde{G}$  in cases where  $\tilde{\chi}_1^\pm$  is the NLSP. Thus, depending on the various possible hierarchies amongst the higgsinos, the following are the possible decay channels of the higgsino-dominated electroweakinos:

$$\begin{aligned}\tilde{\chi}_2^0 &\rightarrow f\bar{f}\tilde{\chi}_1^0, f\bar{f}'\tilde{\chi}_1^\pm, h\tilde{G}, Z\tilde{G} \\ \tilde{\chi}_1^\pm &\rightarrow f\bar{f}'\tilde{\chi}_1^0, f\bar{f}'\tilde{\chi}_2^0, W^\pm\tilde{G} \\ \tilde{\chi}_1^0 &\rightarrow h\tilde{G}, Z\tilde{G}\end{aligned}\tag{3.3.10}$$

where the  $Z$  boson from neutralino decay is mostly longitudinal. The couplings of the neutral higgsinos  $\tilde{\chi}_1^0, \tilde{\chi}_2^0$  and charged higgsino,  $\tilde{\chi}_1^\pm$ , to the gravitino ( $\tilde{G}$ ) LSP are [31]:

$$\begin{aligned}|g_{\tilde{G}\tilde{\chi}_i^0 H_k}|^2 &= |e_k N_{i3} + d_k N_{i4}|^2 (M_{Pl} m_{\tilde{G}})^2, \\ |g_{\tilde{G}\tilde{\chi}_1^\pm H_k^\pm}|^2 &= (|V_{12}^2| \cos\beta + |U_{12}^2| \sin^2\beta) (M_{Pl} m_{\tilde{G}})^2\end{aligned}\tag{3.3.11}$$

for  $i = 1, 2$  corresponding to  $\tilde{\chi}_1^0, \tilde{\chi}_2^0$  and  $k = 1, 2, 3$  corresponding to the CP-even scalars  $h, H$  and CP-odd pseudoscalar  $A$ . The coefficients  $e_k$  and  $d_k$  are as below:

$$\begin{aligned}e_1 &= \cos\alpha, e_2 = -\sin\alpha, e_3 = -\sin\beta \\ d_1 &= -\sin\alpha, d_2 = -\cos\alpha, d_3 = \cos\beta\end{aligned}\tag{3.3.12}$$

and  $N_{ij}$  refer to the  $(ij)^{th}$  entry of the neutralino mixing matrix  $N$ ,  $\alpha$  is the mixing angle between the CP-even Higgses,  $h$  and  $H$ . In the decoupling limit, i.e,  $m_A \gg m_h$ ,  $\beta - \alpha \sim \pi/2$  ( where,  $0 < \beta < \pi$  and  $-\pi < \alpha < 0$  ), the lightest CP-even Higgs ( $h$ ) behaves like the SM Higgs boson [8]<sup>5</sup>. The coupling of the  $Z$  boson to  $\tilde{\chi}_1^0$  and  $\tilde{G}$

---

<sup>5</sup>We assume  $M_A \gg \mu$  for simplicity, therefore disallowing decays of  $\tilde{\chi}_i^0$  to heavy Higgses.



Parameters	$ \mu $ (GeV)	$\text{sign}(\mu)$	$\tan \beta$
Values	0.2-1.5	$\pm 1$	2-45

**Table 1.** Relevant range of the input parameters for the parameter-space scan to study the decay probabilities of the lightest neutralino is shown. We keep other parameters at fixed values which include:  $M_1 = 2$  TeV,  $M_2 = 2$  TeV,  $M_3 = 1.917$  TeV,  $M_{Q_3} = 2.8$  TeV,  $M_{U_3} = 2.8$  TeV,  $M_A = 2.5$  TeV,  $A_t = 3$  TeV and  $m_{\tilde{G}} = 1$  keV.

is as follows:

$$|g_{\tilde{G}\tilde{\chi}_i^0 Z}|^2 = (|N_{11}\sin\theta_W - N_{12}\cos\theta_W|^2 + |N_{i4}\cos\beta - N_{i3}\sin\beta|^2)(M_{Pl}m_{\tilde{G}})^2 \quad (3.3.13)$$

for  $i = 1, 2$ . Thus, the partial decay widths of a higgsino-like neutralino  $\tilde{\chi}_1^0$  are as follows [8, 14, 28]:

$$\Gamma(\tilde{\chi}_1^0 \rightarrow Z\tilde{G}) \propto (|N_{11}\sin\theta_W - N_{12}\cos\theta_W|^2 + \frac{1}{2}|N_{14}\cos\beta - N_{13}\sin\beta|^2)(M_{Pl}m_{\tilde{G}})^2 \quad (3.3.14)$$

$$\Gamma(\tilde{\chi}_1^0 \rightarrow h\tilde{G}) \propto |N_{14}\sin\alpha - N_{13}\cos\alpha|^2(M_{Pl}m_{\tilde{G}})^2 \quad (3.3.15)$$

The terms proportional to  $N_{14}$  and  $N_{13}$  denote the Goldstone couplings; which we discuss in detail later in section 7. In the decoupling limit,  $\sin\alpha = -\cos\beta$  and  $\cos\alpha = \sin\beta$ , thus Equation 3.3.15 reduces to,

$$\Gamma(\tilde{\chi}_1^0 \rightarrow h\tilde{G}) \propto |N_{14}\cos\beta - N_{13}\sin\beta|^2(M_{Pl}m_{\tilde{G}})^2 \quad (3.3.16)$$

For  $|N_{11}|, |N_{12}| \ll |N_{13}|, |N_{14}|$ ,  $\Gamma(\tilde{\chi}_1^0 \rightarrow h\tilde{G}) \sim \Gamma(\tilde{\chi}_1^0 \rightarrow Z\tilde{G})$ . For the higgsino-like  $\tilde{\chi}_1^0$ ,  $N_{13} \simeq N_{14}$  for  $\mu > 0$ , whereas for  $\mu < 0$ , ie,  $N_{13} \sim -N_{14}$  [14]. This leads to an increase in  $\Gamma(\tilde{\chi}_1^0 \rightarrow h\tilde{G})$  as evident from Equation 3.3.16.

## Branching Ratios

We consider a higgsino-like  $\tilde{\chi}_1^0$  as the NLSP with a light  $\tilde{G}$  LSP. As discussed in section 3, the branching ratios of the NLSP are governed by the composition of the NLSP as well as the values of  $\tan\beta$  and  $\mu$ . In Figure 1 we plot the branching ratios of  $\tilde{\chi}_1^0$ 's decay to a  $h\tilde{G}$  or a  $Z\tilde{G}$  as a function of  $\tan\beta$  and  $\mu$ . Among other parameters, the bino, wino and gluino soft mass parameters are  $M_1, M_2, M_3 \sim 2$  TeV respectively, whereas squarks and sleptons masses are kept at  $\sim 2$  TeV. The light stop masses are kept at 2.8 TeV to fit the lightest CP-even Higgs mass in the range 122-128 GeV [32, 33] for  $\mu$  parameter values in the range [0.2:1.5] TeV. The relevant parameter ranges for the scan which is carried out using SPheno-v3.3.6 [34, 35] are summarised in Table 1.

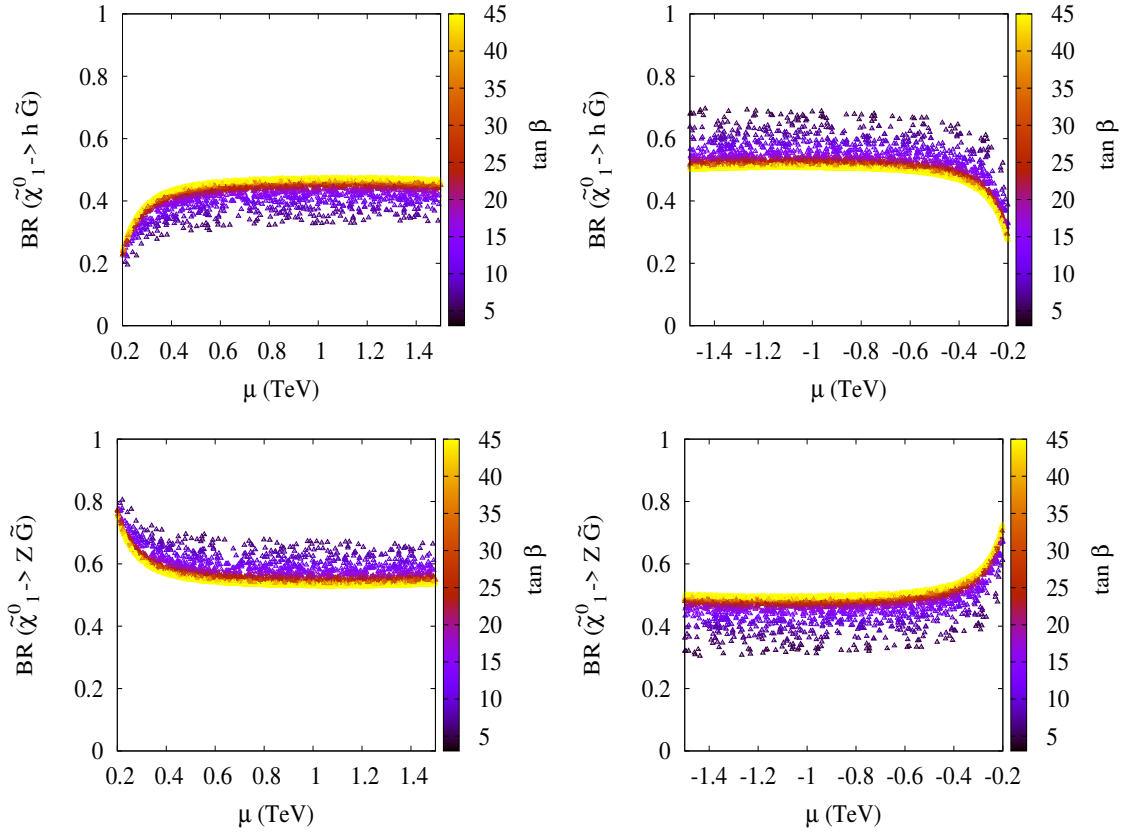


**Figure 1.** Variation of  $\tilde{\chi}_1^0$  to a Higgs (top panel) or  $Z$  boson (bottom panel) along with the  $\tilde{G}$  LSP with  $\mu$  and  $\tan\beta$  in the coloured palette. The parameters of the scan are listed in Table 1.

The decay branching ratios of the higgsino-dominated  $\tilde{\chi}_1^0$  NLSP are governed mainly by values of  $\mu$  and  $\tan\beta$  and hence the composition of the NLSP. Figure 1 clearly shows that there exist three distinct regions of the parameter space, namely the Higgs dominated region, the  $Z$  boson dominated region and the region of parameter space where both the Higgs and the  $Z$  boson modes are comparable. The Higgs dominated  $BR(\tilde{\chi}_1^0 \rightarrow h\tilde{G}) \simeq 0.8$  occurs for negative values of the  $\mu$  parameter whereas the  $Z$  boson dominated  $BR(\tilde{\chi}_1^0 \rightarrow Z\tilde{G}) \simeq 0.8$  is for positive  $\mu$  parameter, both at low  $\tan\beta$  values. In the former case,  $N_{13} = N_{14}$  whereas in the latter case there is a relative sign between  $N_{13}$  and  $N_{14}$  in a small region of the parameter space where the Higgs mode takes over the  $Z$  mode. Although the Higgs mode dominates over the  $Z$  mode throughout the negative  $\mu$  parameter space (see Equation 3.3.16), it decreases with increase in the gaugino admixture in the NLSP at higher values of  $\mu$  and  $\tan\beta$  (as  $\mu$  gets closer to the choice of  $M_1$  and  $M_2$  shown in Table 1), which defines a range of the parameter space with comparable branching ratios for the Higgs and  $Z$  boson decay modes of the  $\tilde{\chi}_1^0$  NLSP. In addition, as the  $\tilde{\chi}_1^0$  becomes more gaugino-like the additional decay mode of  $\gamma\tilde{G}$  would also open up and subsequently

Final State	Production mode	ATLAS	CMS
$2/3/4b + \cancel{E}_T$	$\tilde{\chi}_1^0 \tilde{\chi}_1^\pm, \tilde{\chi}_2^0 \tilde{\chi}_1^\pm, \tilde{\chi}_1^\mp \tilde{\chi}_1^\pm$	[36]	[16]
$\ell^+ \ell^- + \cancel{E}_T$	$\tilde{\chi}_1^0 \tilde{\chi}_1^\pm, \tilde{\chi}_2^0 \tilde{\chi}_1^\pm, \tilde{\chi}_1^\mp \tilde{\chi}_1^\pm$		[16]
$\geq 3\ell + \cancel{E}_T$	$\tilde{\chi}_1^0 \tilde{\chi}_1^\pm, \tilde{\chi}_2^0 \tilde{\chi}_1^\pm, \tilde{\chi}_1^\mp \tilde{\chi}_1^\pm$		[16]
$hh + \cancel{E}_T$	$\tilde{g}\tilde{g}$		[37]
$4\ell + \cancel{E}_T$	$\tilde{\chi}_1^\pm \tilde{\chi}_1^\pm, \tilde{\chi}_1^\pm \tilde{\chi}_2^0$	[38]	
$\geq 2j + \cancel{E}_T$	$\tilde{g}\tilde{g}, \tilde{q}\tilde{q}$	[39]	
$b\bar{b} + \cancel{E}_T$	$\tilde{\chi}_2^0 \tilde{\chi}_1^\pm$	[40]	
$1\ell + b\bar{b} + \cancel{E}_T$	$\tilde{\chi}_2^0 \tilde{\chi}_1^\pm$	[40]	
$3\ell + \cancel{E}_T$	$\tilde{\chi}_2^0 \tilde{\chi}_1^\pm$	[40]	
$\ell^\pm \ell^\pm + \cancel{E}_T$	$\tilde{\chi}_2^0 \tilde{\chi}_1^\pm$	[40]	

**Table 2.** List of experimental searches from LHC relevant for our current study with  $\tilde{G}$  LSP.

dominate the branching probabilities.

## 4 Existing LHC limits

The current bounds on the light higgsinos as NLSP and  $\tilde{G}$  LSP are well studied at LHC for a light gravitino ( $m_{\tilde{G}} = 1$  GeV) assuming prompt decays. The relevant analyses are summarised in Table 2. We discuss in detail the implications of the constraints from LHC on the higgsinos as well as on the strong sector particles as relevant for our study below:

- **Higgsinos:** ATLAS and CMS impose stringent limits on the mass of the higgsinos from searches involving multiple b-jets/leptons along with large missing transverse energy  $\cancel{E}_T$  assuming specific branching probabilities for its decay. The following are the exclusion limits on the higgsino masses [16, 36] :

$$BR(\tilde{\chi}_1^0 \rightarrow h\tilde{G}) \sim 1.0 : m_{\tilde{\chi}_1^0} \geq 880 \text{ GeV (ATLAS); } m_{\tilde{\chi}_1^0} \geq 760 \text{ GeV (CMS).}$$

$$BR(\tilde{\chi}_1^0 \rightarrow Z\tilde{G}) \sim 1.0 : m_{\tilde{\chi}_1^0} \geq 340 \text{ GeV (ATLAS).}$$

Combined exclusion limits on the higgsino mass from multiple searches at CMS are as follows [16]:

$$BR(\tilde{\chi}_1^0 \rightarrow h\tilde{G}) \sim 1.0 : m_{\tilde{\chi}_1^0} \geq 775 \text{ GeV (CMS).}$$

$$BR(\tilde{\chi}_1^0 \rightarrow Z\tilde{G}) \sim 1.0 : m_{\tilde{\chi}_1^0} \geq 650 \text{ GeV (CMS).}$$

- **Strong Sector:** Direct limits for a massless gravitino LSP scenario are placed on strong sector particles with  $\tilde{G}$  LSP from opposite-sign dilepton + missing

energy searches in ATLAS [41] excluding  $m_{\tilde{g}} \geq 1.8$  TeV for  $m_{\tilde{\chi}_1^0} < 600$  GeV. Stringent limits also arise from boosted Higgs searches [42] interpreted in terms of a simplified scenario with a light  $\tilde{\chi}_1^0$  LSP excluding  $m_{\tilde{g}} \geq 2.2$  TeV for  $m_{\tilde{\chi}_1^0} = 1$  GeV. Other indirect searches which constrain the above mentioned scenario are multi-jets and/or multileptons +  $\cancel{E}_T$  searches [38, 39], owing to the presence of  $h/Z$  from the NLSP decay which give rise to leptons or jets in the final state.

## 5 Benchmarks for our analysis

We choose representative benchmark points of the allowed parameter space to probe a low-lying higgsino-like  $\tilde{\chi}_1^0$  NLSP with light  $\tilde{G}$  LSP, focusing primarily on promptly decaying  $\tilde{\chi}_1^0$  signals. Our choice of benchmarks are motivated by the underlying aim of uncovering the characteristics of a higgsino-like  $\tilde{\chi}_1^0$  NLSP in the presence of a light  $\tilde{G}$  LSP. Decays of the strong sector particles occur via the following decay modes for a keV  $\tilde{G}$ : for gluinos, with squarks and electroweakinos decoupled, the possible decay modes to the NLSP,

$$\tilde{g} \rightarrow t\bar{t}\tilde{\chi}_1^0, \quad b\bar{b}\tilde{\chi}_1^0, \quad t\bar{b}\tilde{\chi}_1^-, \quad q\bar{q}\tilde{\chi}_1^-, \quad q\bar{q}\tilde{\chi}_1^0$$

Among these decay modes, owing to the higgsino-like nature of the NLSP, the interaction strengths are governed by the Yukawa couplings. Hence the third generation squark channels dominate. Whereas for the first and second generation squarks, the possible decay modes are:

$$\tilde{q} \rightarrow q\tilde{\chi}_1^0, \quad q\tilde{\chi}_2^0, \quad q'\tilde{\chi}_1^\pm$$

As discussed in section 3, the dominant decay mode of the  $\tilde{\chi}_1^0$  NLSP is to either a Higgs or a  $Z$  boson along with the  $\tilde{G}$  LSP which contributes to the missing energy. This is because, for a keV  $\tilde{G}$  the sparticles decay primarily to the  $\tilde{\chi}_1^0$  NLSP, either directly or via cascade decays through the intermediate sparticles [43]. We wish to study the collider prospects of observing the final state:  $\geq 1b + \ell^+\ell^- + \cancel{E}_T$  in the context of the upcoming high luminosity run of the LHC and explore kinematic variables reflecting the composition of the NLSP. We discuss below the characteristic features of each of the chosen benchmarks which follow:

- Squarks and keV  $\tilde{G}$  (**BP1**) with higgsino-like  $\tilde{\chi}_1^0$  NLSP.
- Squarks and keV  $\tilde{G}$  (**BP2**) with gaugino-like  $\tilde{\chi}_1^0$  NLSP.
- Light higgsinos only and keV  $\tilde{G}$  (**BP3**) with  $\tilde{\chi}_1^0$  NLSP.
- Squarks and keV  $\tilde{G}$  (**BP4**) with a heavy gaugino-higgsino mixed  $\tilde{\chi}_1^0$  NLSP.

For simplicity,  $M_1, M_2 \sim 2.3 - 2.4$  TeV such that their contribution directly or via cascade decays of strong sector sparticles to the signal region under study is negligible. Among the constraints on the parameter space, light Higgs mass is within the range 122-128 GeV [32, 33]. In all cases, both  $\tilde{t}_1$  and  $\tilde{t}_2$  are heavy or the trilinear coupling,  $A_t$ , is large to fit the lightest CP-even Higgs mass,  $m_h$  in the range 122-128 GeV [32, 33, 44]. Also,  $m_{\tilde{\chi}_1^\pm}$  adheres to LEP limit of 103.5 GeV [45]. We focus primarily on the following cases:

- **BP1:** We choose this benchmark with squark lighter in mass than the gluinos, i.e,  $m_{\tilde{q}} = 2.3$  TeV while  $m_{\tilde{g}} \sim 2.8$  TeV respectively. We choose  $\mu = 800$  GeV and  $\tan\beta = 25$  such that  $BR(\tilde{\chi}_1^0 \rightarrow h\tilde{G}) \sim 0.45$  whereas  $BR(\tilde{\chi}_1^0 \rightarrow Z\tilde{G}) \sim 0.55$ . The lightest chargino,  $\tilde{\chi}_1^\pm$  decays primarily via  $\tilde{\chi}_1^0$ , i.e,  $BR(\tilde{\chi}_1^\pm \rightarrow f\bar{f}'\tilde{\chi}_1^0) \sim 0.98$ .
- **BP2:** This benchmark is quite similar to **BP1** except with a major difference in the composition of the NLSP. Here the  $\tilde{\chi}_1^0$  NLSP is dominantly zino-like, i.e,  $M_1 = M_2 = 800$  GeV and  $\mu = 2$  TeV. Thus,  $\tilde{\chi}_1^0 \rightarrow \gamma\tilde{G} \sim 0.75$  and  $\tilde{\chi} \rightarrow Z\tilde{G} \sim 0.25$ . The sole pupose of choosing this benchmark is to compare the difference in distributions referred to in section 7 which gives a clear indication of the NLSP composition. Note that the dominant signal for this benchmark is via hard photon signals along with jets and large missing energy, which was studied in our earlier work [43].
- **BP3:** For this benchmark we consider a more simplified spectra with only a light higgsino sector where we have decoupled squarks and gauginos by making them ultra heavy and out of reach of the LHC. To achieve this we choose  $\mu = 700$  GeV whereas  $M_1, M_2 \sim 7$  TeV and  $M_3, M_Q \sim 7$  TeV. We have chosen  $\tan\beta = 25$  which gives a  $BR(\tilde{\chi}_1^0 \rightarrow h\tilde{G}) \sim 0.45$  and  $BR(\tilde{\chi}_1^0 \rightarrow Z\tilde{G}) \sim 0.55$  as in **BP1**.
- **BP4:** We choose here an overall heavy spectra with a significantly heavier NLSP with  $\mu = 2.2$  TeV and with  $M_1, M_2 = 2.3$  TeV. This makes the electroweakinos out of direct reach of LHC but accessible via cascades of strongly produced squarks which are around 2.3 TeV too. This benchmark also ensures a large gaugino-higgsino admixture in the  $\tilde{\chi}_1^0$  as compared to **BP1** which can test the efficacy of our analysis in unravelling the composition of the NLSP.

Finally we also include a benchmark **BP5** similar to **BP1** with a larger branching fraction into the Higgs boson and gravitino mode which would represent the low  $\tan\beta$  and negative  $\mu$  region of the parameter space. We choose the benchmarks after passing them through the public software **CheckMATE** [46]. Among the searches implemented in **CheckMATE**, stringent constraints come from multijet searches by

Parameters	BP1	BP2	BP3	BP4	BP5
$M_1$	2400	800	7000	2300	2400
$M_2$	2400	800	7000	2300	2400
$\mu$	800	2400	700	2250	-800
$\tan \beta$	25	25	25	25	3.8
$A_t$	3200	3200	100	3200	3740
$m_A$	2500	2500	2500	2500	3000
$m_h$	125.3	125.3	127.1	124.5	122.2
$m_{\tilde{g}}$	2806.4	2807.1	7271.2	2840.1	2663.3
$m_{\tilde{q}_L}$	2303.3	2300.2	7156.4	2313.3	2280.6
$m_{\tilde{q}_R}$	2302.2	2302.5	7155.4	2312.5	2283.7
$m_{\tilde{t}_1}$	2357.5	2184.8	7057.0	2509.1	1581.1
$m_{\tilde{t}_2}$	2340.9	2370.8	7104.0	2666.0	2271.4
$m_{\tilde{b}_1}$	2260.9	2266.4	7102.2	2583.4	2237.5
$m_{\tilde{b}_2}$	2299.0	2323.9	7129.0	2630.3	2295.6
$m_{\tilde{l}_L}$	3331.8	3326.8	7337.2	3332.6	3329.4
$m_{\tilde{l}_R}$	3335.6	3333.7	7336.3	3336.3	3334.1
$m_{\tilde{\chi}_1^0}$	810.9	797.9	718.8	2211.0	1214.8
$m_{\tilde{\chi}_2^0}$	-814.4	837.8	-723.7	-2254.8	-1217.2
$m_{\tilde{\chi}_1^\pm}$	812.5	837.9	720.9	2223.1	1216.4
$m_{\tilde{\chi}_2^\pm}$	2415.7	2397.3	1925.9	2350.5	2420.9
$m_{\tilde{\chi}_3^0}$	2386.3	-2394.8	1923.6	2290.1	2392.2
$m_{\tilde{\chi}_4^0}$	2415.6	2397.4	1925.8	2350.5	2420.9
$m_{\tilde{G}} \text{ (keV)}$	1.0	1.0	1.0	1.0	1.0
$BR(\tilde{\chi}_1^0 \rightarrow h\tilde{G})$	0.45	0.0	0.44	0.23	0.27
$BR(\tilde{\chi}_1^0 \rightarrow Z\tilde{G})$	0.55	0.25	0.56	0.75	0.73
$BR(\tilde{\chi}_1^0 \rightarrow \gamma\tilde{G})$	0	0.75	0	0.02	0
$BR(\tilde{\chi}_1^\pm \rightarrow W\tilde{G})$	0.024	0.0	0.003	0.0001	0.15
$BR(\tilde{\chi}_1^\pm \rightarrow W^*\tilde{\chi}_1^0)$	0.976	1.0	0.997	0.9999	0.85

**Table 3.** List of benchmarks chosen for our study. Mass parameters are in GeV unless specified otherwise.

ATLAS [39]. The benchmark points are generated using the spectrum generator SPheno-v3.3.6 [34, 35] and shown in Table 3.

## 6 LHC Signals

We now discuss in detail the possible LHC signals arising in the current scenario with a higgsino-like  $\tilde{\chi}_1^0$  NLSP and keV  $\tilde{G}$  LSP. Strong sector sparticles pair produced

at  $\sqrt{s} = 13$  TeV LHC cascade down to the  $\tilde{\chi}_1^0$  NLSP along with additional jets arising from the cascade. In situations where the strong sector is not kinematically accessible, it is worthwhile to explore signals from the direct production of the low-lying higgsinos decaying promptly to the NLSP  $\tilde{\chi}_1^0$  which then further decays to a Higgs/ $Z$  gauge boson and the  $\tilde{G}$  LSP. As discussed in section 3, such a scenario would lead to  $hh/hZ/ZZ$  final states with/without extra hard jets arising from the strong sector cascade.

Motivated by the characteristics of a higgsino NLSP spectra, among the multifarious signatures possible we focus on a final state consisting of a Higgs and  $Z$  boson along with large  $\cancel{E}_T$  as the primary signature of such a scenario. Although both Higgs and  $Z$  dominantly decay to hadronic final states, (i.e,  $BR(h \rightarrow b\bar{b}) \sim 0.58$  and  $BR(Z \rightarrow jj) \sim 0.67$ ), the corresponding hadronic background would be clearly overwhelming for the all hadronic signal. In addition, to study the characteristic polarization of the  $Z$  boson coming from the decay of the NLSP we require an efficient and cleaner mode of reconstruction which can only come through the leptonic decay of the weak gauge boson. We therefore choose a final state that includes atleast one  $b$ -jet and two same flavour opposite-sign leptons along with  $\cancel{E}_T$ . Owing to the presence of leptons in the final state, this is a relatively clean channel to observe at LHC as compared to an all hadronic final state. Since the LSP is a very light  $\tilde{G}$ , the ensuing  $h/Z$  from the NLSP decay and hence, the  $b$ -jets and/or leptons have large transverse momentum ( $p_T$ ), thereby leading to a large  $\cancel{E}_T$ , where  $\vec{\cancel{E}}_T = -\vec{p}_{T_{vis}}$  (balancing the net transverse momenta,  $\vec{p}_{T_{vis}}$  of the visible particles). No specific criteria is imposed on the number of light jets in the scenario as will be present if the signal arises from the decay of the squarks or gluinos to the NLSP. This is because our choice of an inclusive final state signal would be able to highlight the presence of a higgsino-like NLSP irrespective of the rest of the underlying MSSM spectrum, *i.e.* with/without the strong sector placed above the low-lying higgsinos.

### Signal, Background and Event selection criteria

We consider the following SUSY production processes involving the first and second generation squarks as well as the low-lying higgsinos to be pair produced when kinematically accessible:

$$pp \rightarrow \tilde{q}_i \tilde{q}_j, \tilde{q}_i \tilde{q}_j^*, \tilde{q}_i^* \tilde{q}_j^*, \tilde{\chi}_1^0 \tilde{\chi}_2^0, \tilde{\chi}_1^\pm \tilde{\chi}_1^0, \tilde{\chi}_1^\pm \tilde{\chi}_2^0, \tilde{\chi}_1^\pm \tilde{\chi}_1^\pm$$

For a keV  $\tilde{G}$  LSP with substantial mass difference between the NLSP and LSP, the following decay modes are in order:

$$\begin{aligned} \tilde{q} &\rightarrow q \tilde{\chi}_1^0, & \tilde{\chi}_1^0 &\rightarrow h/Z \tilde{G} \\ \tilde{q} &\rightarrow q \tilde{\chi}_2^0, & \tilde{\chi}_2^0 &\rightarrow f \tilde{f} \tilde{\chi}_1^0 \\ \tilde{q} &\rightarrow q' \tilde{\chi}_1^\pm, & \tilde{\chi}_1^\pm &\rightarrow f \tilde{f}' \tilde{\chi}_1^0 \end{aligned}$$

where  $f$  and  $f'$  refer to the SM fermions. Thus when the signal is generated from the pair production of the strongly interacting sparticles, the final state consists of at least two hard jets in the  $hh/hZ/ZZ$  final state along with a pair of invisible gravitinos which contribute to the large  $\cancel{E}_T$ . Among the possible combinations of the decay products of  $h$  and  $Z$ , we primarily focus on the  $\geq 1b + \ell^+\ell^-$  final state along with  $\cancel{E}_T$ . Since the  $Z$  decays leptonically, it gives a cleaner channel and better control over the SM backgrounds as compared to a hadronic final state.

We generate the signal events in **Madgraph\_v5** [47] using the model UFO files available from **Feynrules** [48]. Subsequently, parton level events are showered and hadronised using **Pythia** [49, 50] and detector simulation is performed using **Delphes** [51]. Jets (including b-jets) are reconstructed using the anti- $k_T$  algorithm [52] using **Fastjet** [53] with minimum transverse momentum,  $p_T > 20$  GeV within a cone  $\Delta R = 0.4$ . Charged leptons are reconstructed in a cone of  $\Delta R = 0.2$  with a maximum energy deposit in the cone from all other particles limited to 10% of the  $p_T$  of the lepton. The significant contributions to the SM background for the given final state come from

- $t\bar{t}$ , ( $t \rightarrow bW^+$ ,  $W^+ \rightarrow \ell^+\nu$ )
- $hZ$  + jets, ( $h \rightarrow b\bar{b}$ ,  $Z \rightarrow \ell^+\ell^-$ )
- $t\bar{t}Z$ , ( $Z \rightarrow \ell^+\ell^-$ )
- $ZZ$ , ( $Z \rightarrow b\bar{b}$ ,  $Z \rightarrow \ell^+\ell^-$ )
- $W^\pm W^\pm Z$ , ( $Z \rightarrow \ell^+\ell^-$ )
- $Zb\bar{b} + \cancel{E}_T$ , ( $Z \rightarrow \ell^+\ell^-$ )

Although the QCD background has a large cross-section, they have negligible contribution to the signal region characterized by large  $\cancel{E}_T$  as well as effective mass,  $M_{Eff}$  which helps probe the heavy mass scale of the SUSY particles and would serve as an effective discriminator between the SUSY signal and SM background. For SM background, we have performed showering and hadronisation using **Pythia** [49, 50] and perform MLM matching [47] when needed with  $QCUT=20-30$  GeV.

### Primary selection criteria

We choose the following basic selection criteria to identify leptons ( $e^-$ ,  $\mu^-$ ) and (b)-jets in the signal and background:

- The charged leptons are identified with  $p_T > 10$  GeV and  $|\eta| < 2.5$ .
- All reconstructed jets and b-jets have  $p_T > 30$  GeV and  $|\eta| < 2.5$ .
- Jets and leptons are isolated with  $\Delta R_{ij} > 0.4$  and  $\Delta R_{\ell\ell} > 0.2$ .



## Signal Analysis

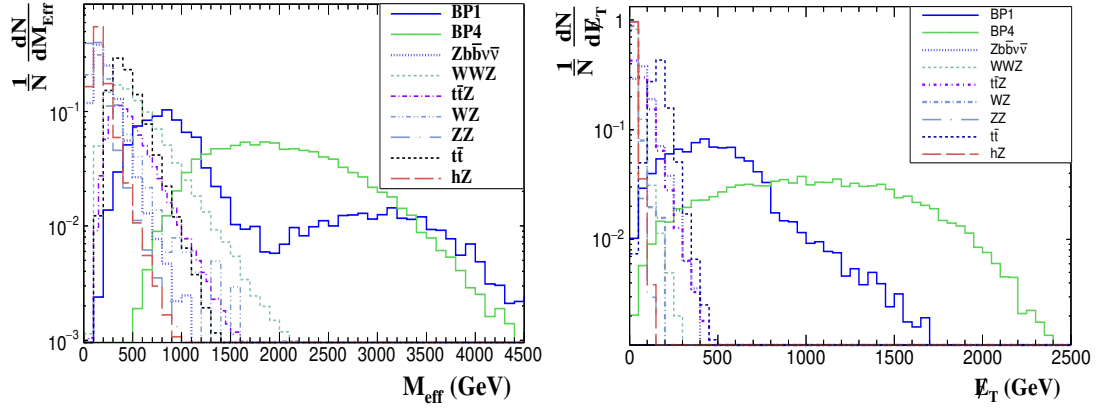
We look at final states with atleast one  $b$ -jet and a pair of opposite-sign same flavour leptons ( $e^-$ ,  $\mu^-$ ) along with large  $\cancel{E}_T$  carried away by the LSP. We also veto events with a photon with  $p_T > 10$  GeV and  $|\eta| < 2.5$ . The missing transverse energy,  $\cancel{E}_T = |\vec{p}_{T_{vis}}|$ , where  $\vec{p}_{T_{vis}} = \sum_j \vec{p}_T(j) + \vec{p}_T(\ell^+) + \vec{p}_T(\ell^-)$  is the net transverse momentum of the signal ( $b$ )-jets and charged leptons in the final state. Since the NLSP-LSP mass gap is large, the transverse momenta carried by the decay products are large thereby ensuring a large amount of  $\cancel{E}_T$  in the event.

Figure 2 shows the normalized differential distribution of a few kinematic variables ( $M_{Eff}$  and  $\cancel{E}_T$ ) for **BP1** and **BP4** along with the background. The SUSY signal distributions for the missing transverse energy ( $\cancel{E}_T$ ) and effective mass ( $M_{Eff}$ ) are widely separated from the SM background for **BP4** in the presence of a heavy NLSP. However the signal events peak at a much lower value  $\sim 600$  GeV for **BP1** while significant events of the signal are found at large  $M_{Eff}$  values  $\sim 2.0$  TeV for **BP4**. Note that for **BP4** this is due to the high transverse momentum of the jets, and leptons arising from the decay cascades of the heavy  $\mathcal{O}(2)$  TeV range sparticles. However for **BP1** with a light NLSP, there is considerable overlap of the kinematic distributions with the background while differing in the tail of the distribution. This happens because the dominant contribution to the signal comes from the direct production of the light higgsino sector as compared to the strong production cross-section. We break our analysis in two parts to study different scenarios that can present itself at LHC. The signal from a heavy spectrum of  $\mathcal{O}(2)$  TeV including the NLSP, that can only have relevant signal contribution through the production of strongly interacting sparticles at the LHC is optimised using cuts in **Analysis 1** while the signal for relatively lighter electroweakino states being directly accessible at LHC with smaller contributions from the strong sector is analysed in **Analysis 2**. Appropriate cuts on the relevant kinematic variables will be crucial to remove SM background in the subsequent collider analyses to study the two scenarios discussed above.

### Analysis 1

As a crucial part of our analysis is dependent on the reconstruction of the  $Z$  boson in the events through the dilepton mode, the event rate for the signal will suffer due to the small branching fraction of the gauge boson to charged leptons. In addition, if we intend to reconstruct the light Higgs boson too using double  $b$ -tag jets, we will end up restricting our search sensitivity significantly. We therefore need to select events using proper cuts to be able to identify the  $Z$  boson as well as imply a Higgs like event. In order to select such a final state we implement the following event selection criterion to retain a significant amount of signal against the SM background:

- **D1:** We select a final state with upto two opposite sign leptons of same flavour ( $N_\ell = 2$  with  $p_T > 20$  GeV) and atleast one  $b$ -jet with  $p_T > 30$  GeV.



**Figure 2.** Distribution of few useful kinematic variables before application of any selection cuts.

- **D2:** To reconstruct the  $Z$  boson we demand that the invariant mass of a dilepton pair (opposite-sign same-flavour) in the signal events is within the  $Z$  mass window satisfying  $76 < M_{\ell^+\ell^-} < 106$  GeV.

Another kinematic variable of importance is the *transverse* mass  $M_{T_2}$  [54]. It is reconstructed using the leading and sub-leading lepton  $p_T$  along with  $\cancel{E}_T$ . For SM processes such as  $t\bar{t}$ ,  $M_{T_2}$  shows an end point value  $\sim M_W$ , the mass of the  $W$  boson decaying leptonically thereby yielding an invisible neutrino. For SUSY processes, the end-point is determined by the mass difference between the NLSP and LSP. For a light keV scale LSP and TeV NLSP, the end-point is large compared to  $M_W$  and can serve as an effective discriminator between SUSY signals and the dominant SM background subprocesses.

- **D3:** We demand a cut on the kinematic variable  $M_{T_2} > 90$  GeV to remove backgrounds from  $t\bar{t}$ .

An important kinematic variable is the effective mass,  $M_{Eff} = p_T(\ell^+) + p_T(\ell^-) + \cancel{E}_T + \sum p_{T_i}(j)$ , the scalar sum of the transverse momenta of the visible jets, leptons and  $\cancel{E}_T$  in the event.  $M_{Eff}$  reflects the mass scale of the heavy SUSY particles and hence is an efficient variable to suppress SM background. However a strong cut on  $M_{Eff}$  would choose to retain contributions from a very heavy spectrum and therefore in this case we focus on the benchmarks that contribute mainly through the production of the strong sector sparticles, *viz.* **BP4** and **BP5**. Note that the strong sector for **BP1** is of similar value to **BP4** and **BP5** and therefore the signal rates coming from the strong sector would be very similar. However, as the dominant fraction of signal events would be from the light higgsino production, the below given cuts are not particularly optimised to study **BP1** while **BP3** signal becomes very small. We shall discuss these benchmarks in **Analysis 2**.

- **D4**: Since nearly all the SUSY particles except LSP are very heavy for **BP4** and **BP5**, a large  $M_{Eff}$  is expected for the signal over the SM background as shown in Figure 2. We therefore demand a strong cut of  $M_{Eff} > 2$  TeV. This cut renders the signal for other benchmarks to a relatively smaller value.
- **D5**: In addition we also put a strong cut on missing transverse energy,  $\cancel{E}_T > 300$  GeV to further remove remaining contributions from SM background processes.

Signal	<b>D1</b>	<b>D2</b>	<b>D3</b>	<b>D4</b>	<b>D5</b>
<b>BP1</b>	112	92	81	24	21
<b>BP3</b>	98	83	74	2	2
<b>BP4</b>	15	12	12	10	10
<b>BP5</b>	24	17	15	15	14
SM Background	<b>D1</b>	<b>D2</b>	<b>D3</b>	<b>D4</b>	<b>D5</b>
$t\bar{t}$	365125	64968	186	-	-
$hZ$	29348	28360	781	1.76	0.16
$ZZ$	178581	172636	2124	15	2.3
$t\bar{t}Z$	3043.3	2111	287	6.14	0.98
$t\bar{t}W$	9121	1802	13.6	-	-
$WWZ$	159	153	13	0.65	0.074
Total Background					3

**Table 4.** Number of signal and background events for  $\geq 1 b + \ell^+ \ell^- + \cancel{E}_T$  at  $\sqrt{s} = 13$  TeV LHC for  $\mathcal{L} = 3000 \text{ fb}^{-1}$  using cuts **D1-D5**. Note that the events have been rounded-off to the nearest integer. Cross-sections for SUSY signals have been scaled using NLO K-factors [55] and wherever available, NLO+NLL K-factors [56]. Cross-sections for SM background processes have been scaled using NLO K-factors [47] and wherever available, NNLO K-factors [57–61] have been used.

We show the cut-flow result of our analysis for the signal and SM background in Table 4. As expected the signal rates coming from a 2 TeV squark sector yields quite small numbers, even with an integrated luminosity of  $3000 \text{ fb}^{-1}$ . The overwhelmingly huge SM background is brought in control by primarily using the  $M_{T_2}$  cut and is then rendered negligibly small using the combination of  $M_{Eff}$  and  $\cancel{E}_T$  cuts. We find that the sequence of cuts shown in Table 4 affects the signal slightly with a suppression of the signal rate of less than 50% for **BP4** and **BP5**. Thus we find a significant number of SUSY signal events surviving the event selection. Note that while a large suppression of signal events happens for **BP1** it is still quite large compared to the SM background, unlike that for **BP3**.

We compute the statistical significance ( $\mathcal{S}$ ) of the above signals using the formula in Eq. 6.6.1 and show the required integrated luminosities to observe and discover

the signal in Table 5:

$$\mathcal{S} = \sqrt{2 \times \left[ (s+b) \ln\left(1 + \frac{s}{b}\right) - s \right]}. \quad (6.6.1)$$

where  $s$  and  $b$  refer to the number of signal and background events respectively. We observe that benchmarks **BP4** and **BP5** require large integrated luminosities

Benchmark	$\mathcal{L}$ (in $fb^{-1}$ ) for $3\sigma$ excess	$\mathcal{L}$ (in $fb^{-1}$ ) for $5\sigma$ excess
<b>BP1</b>	508	1409
<b>BP4</b>	1647	4575
<b>BP5</b>	956	2654

**Table 5.** Required luminosities for observing the SUSY signal for the different benchmarks at  $\sqrt{s} = 13$  TeV LHC run.

whereas **BP3** with a decoupled squark sector is out of reach of LHC. Although **BP1** is observable at LHC, the large  $M_{Eff}$  cut reduces the contribution from the light higgsino sector which is directly accessible at LHC. Therefore, this analysis is more sensitive to the case of heavier spectra that also includes the NLSP to be quite heavy, such as **BP4** and **BP5**. However with a light higgsino sector and similar squark masses to **BP4** such as in **BP1** we are still able to get a relatively healthy number for the signal albeit after losing a large part of the signal events. A more optimised set of cuts is used in **Analysis 2** to study the scenario with lighter NLSP mass.

Note that for simplicity we have looked at the presence of light squarks in the spectrum. Significant contribution to the signal region under study may also arise in the presence of gluinos from a compressed  $\tilde{q}\tilde{g}$  sector mainly from squark-gluino associated production. The gluinos decay via the NLSP leading to a large number of b-jets in the final state besides the contribution from the NLSP decay to the LSP. Since we have studied an inclusive final state,  $\geq 1b + \ell^+\ell^- + \cancel{E}_T$ , the contribution from the gluino will enhance the SUSY signal cross-section. We also comment on the prospect of multijet searches as discovery channels for our scenario. Using the SM backgrounds of the multijet analyses [39] we estimate the reach of the squark masses to be 2.78 TeV to achieve a  $5\sigma$  discovery at an integrated luminosity of  $3000 \text{ fb}^{-1}$  at LHC. For such heavy spectra the final state channel of  $\geq 1b + \ell^+\ell^- + \cancel{E}_T$  would not be within the LHC reach and therefore multijet channel would be the best discovery channel.

## Analysis 2

We now focus on the signal contribution arising dominantly from the electroweak sector of sparticles with/without the strong sector when accessible, as for benchmark

**BP1** and **BP3**. Since the electroweakino sector is lighter, a strong cut on  $M_{Eff}$  as used in **D4** will deplete the signal significantly in this case. Therefore, we employ a different set of cuts for investigating the signal region  $\geq 1\ b + \ell^+ \ell^- + \cancel{E}_T$  arising from the low-lying higgsino sector. We consider the contributions from the electroweak sector in addition to the strong sector for the benchmarks in our study when they are kinematically accessible and study the benchmarks **BP1** and **BP3**. The following cuts are implemented on both signal and background:

- **E1:** As in **Analysis 1**, we select a final state with upto two opposite sign leptons of same flavour ( $N_\ell = 2$  with  $p_T > 20$  GeV) and atleast one  $b$ -jet with  $p_T > 30$  GeV.
- **E2:** To reconstruct the  $Z$  boson we demand that the invariant mass of the dilepton pair in the signal events is within the  $Z$  mass window satisfying  $76 < M_{\ell^+ \ell^-} < 106$  GeV.
- **E3:** As before,  $M_{T_2}$  is an efficient cut to reduce background contributions from  $t\bar{t}$  to the signal region. We demand a slightly stronger cut of  $M_{T_2} > 120$  GeV in this case as it helps improve the signal-to-background ratio.
- **E4:** The large mass scales of SUSY particles again lead to a higher  $M_{Eff}$  as compared to the backgrounds. Since  $\mu \sim 700 - 800$  GeV,  $M_{Eff} > 300$  GeV helps reduce background dominantly compared to signal.
- **E5:** The SUSY signal has a larger  $\cancel{E}_T$  as compared to the SM background. Hence  $\cancel{E}_T > 300$  GeV cut helps reduce a significant part of the remnant contributions from SM background.

The cut-flow table for the signal and SM background are as shown in Table 6. Since the higgsinos, with masses in the range  $\mu = 700 - 800$  GeV are rather light compared to the heavy squarks, a large cut on variables such as  $M_{Eff} \sim 2$  TeV is quite ineffective to search for a spectrum with a lighter higgsino sector since the signal will be depleted significantly. Therefore, in this case we rely on a much relaxed cuts on  $M_{Eff}$  and a slightly stronger cut on  $M_{T_2}$  to ensure substantial removal of the  $t\bar{t}$  background while retaining the signal events. However other background contributions remain with a softer  $M_{Eff}$  cut such as that from  $Zb\bar{b} + \cancel{E}_T$ . This still gives a significantly large event rate for the signal as compared to **Analysis 1** and thereby allowing a  $\sim 8.6(10)\sigma$  discovery possible with  $\mathcal{L} = 3000\ fb^{-1}$ . Since both the benchmarks have similar branching fractions into the  $Z$  and Higgs mode, the difference in the required integrated luminosity is primarily owing to the fact that the NLSP mass is heavier in **BP1** than in **BP3**. The required luminosity for observing a  $3\sigma$  and  $5\sigma$  significance at LHC are shown Table 7. We conclude that both **BP1** and **BP3** are well within the discovery reach of the high luminosity run of LHC.

<b>BP1</b>	<b>E1</b>	<b>E2</b>	<b>E3</b>	<b>E4</b>	<b>E5</b>
$\tilde{\chi}_1^\pm \tilde{\chi}_1^\pm$	16	13	11	11	9
$\tilde{\chi}_1^\pm \tilde{\chi}_{1/2}^0$	65	54	47	47	36
$\tilde{\chi}_2^0 \tilde{\chi}_1^0$	16	14	12	12	9
$\tilde{q}\tilde{q}$	30	24	19	19	18
Total					73
<b>BP3</b>	<b>E1</b>	<b>E2</b>	<b>E3</b>	<b>E4</b>	<b>E5</b>
$\tilde{\chi}_1^\pm \tilde{\chi}_1^\pm$	33	27	24	24	18
$\tilde{\chi}_1^\pm \tilde{\chi}_{1/2}^0$	126	107	87	87	65
$\tilde{\chi}_2^0 \tilde{\chi}_1^0$	33	28	24	24	18
Total					101
<b>SM Background</b>	<b>E1</b>	<b>E2</b>	<b>E3</b>	<b>E4</b>	<b>E5</b>
$t\bar{t}$	365125	64968	-	-	-
$hZ$	29348	28360	298	298	0.67
$ZZ$	178581	172636	774	774	6.61
$t\bar{t}Z$	3043	2111	151	151	8.6
$t\bar{t}W$	9121	1802	1	1	-
$WWZ$	159	153	6	6	0.23
$Zb\bar{b} + \cancel{E}_T$	2933	2905	312	311	34.7
Total					51

**Table 6.** Number of signal and background events for  $\geq 1 b + \ell^+ \ell^- + \cancel{E}_T$  at  $\sqrt{s} = 13$  TeV LHC for  $\mathcal{L} = 3000 \text{ fb}^{-1}$  using cuts **E1-E5**. Note that the events have been rounded-off to the nearest integer. Cross-sections for SUSY signals have been scaled using NLO K-factors [55] and wherever available, NLO+NLL K-factors [56]. Cross-sections for SM background processes have been scaled using NLO K-factors [47] and wherever available, NNLO K-factors [57–61] have been used.

Benchmark	$\mathcal{L}$ (in $fb^{-1}$ ) for $3\sigma$ excess	$\mathcal{L}$ (in $fb^{-1}$ ) for $5\sigma$ excess
<b>BP1</b>	373	1034
<b>BP3</b>	208	577

**Table 7.** Required luminosities for observing the SUSY signal for the different benchmarks at  $\sqrt{s} = 13$  TeV LHC run.

We now are set to study the efficacy of the signal that we have analysed to identify the nature of the NLSP and its inherent composition with respect to the gaugino-higgsino admixture in the following section.

## 7 A Distinguishing Feature: Longitudinal vs Transverse Gauge bosons

The Goldstone boson equivalence theorem states that, at very high energies, i.e.,  $\sqrt{s} \gg m_V$ , (where  $V = W^\pm, Z$ ), the weak gauge bosons may be approximated by their longitudinal polarisation mode (with corrections upto factors  $\frac{M_V}{E_V}$ , where mass  $M_V$  and energy  $E_V$  are the mass and energy of the gauge bosons respectively). In this limit,  $W^\pm, Z$  bosons are primarily produced in the transverse polarised state for SM processes. This is because for SM gauge bosons, couplings of the longitudinal modes are suppressed by factors  $M_V/E_V$  at high energies (since  $E_V \gg M_V$  for  $V = W^\pm, Z$ ). However vector bosons arising from decay of heavy particles (say,  $X$  where  $X$  may be a heavy Higgs, or heavy gauge boson or heavy fermion) have enhanced couplings of the longitudinal mode by factors  $(M_X/M_W)^2$  [62]. Therefore distinguishing the properties of longitudinal gauge bosons from SM processes giving rise to dominantly transverse gauge bosons is a clear signature of Beyond Standard Model (BSM) scenarios.

After electroweak symmetry breaking, the three massless Goldstone bosons are absorbed by the  $W^\pm$  and  $Z$  bosons contributing to their longitudinal modes. The other five degrees of freedom form the physical Higgs bosons:  $h, H, A^0$  and  $H^\pm$ . From section 3, we observe that there exists a substantial parameter space where the decay of the higgsino into a  $Z$  and gravitino is comparable to the decay branching into a Higgs and gravitino as also discussed in earlier works [14, 15]. Since the Goldstone boson from the Higgs doublet (which obtains a *vev* after electroweak symmetry breaking) is responsible for the longitudinal component of the  $Z$  boson, a higgsino-like NLSP decays predominantly to a longitudinally polarised  $Z$  boson. This is evident from Equation 3.3.14, where for a higgsino-like NLSP,  $|N_{13}|, |N_{14}| \gg |N_{11}|, |N_{12}|$ . The higgsino fractions thus drive the  $\tilde{\chi}_1^0 \rightarrow Z\tilde{G}$  decay, where  $Z$  is dominated by the neutral Goldstone boson. It is important to note that the polarisation information of such a  $Z$  boson can be a signature for the presence of a higgsino-like  $\tilde{\chi}_1^0$ . Conversely, for a gaugino-like NLSP (a photino or zino-like)  $\tilde{\chi}_1^0$  NLSP,  $|N_{11}|, |N_{12}| \gg |N_{13}|, |N_{14}|$ , thereby leading to a dominantly transverse  $Z$  boson being produced from the NLSP decay. Thus, the polarisation of the  $Z$  boson could be an efficient discriminator between a higgsino-like and gaugino-like NLSP.

Although our focus is on the polarisation of  $Z$  boson in the context of SUSY in this work, the polarisation information of vector bosons may be extremely useful even for non-SUSY scenarios where a polarised gauge boson is likely to be produced from the decay of a heavy particle. Thus, the features of the longitudinal  $Z$  boson which will be discussed in detail in this work are also applicable for other scenarios as well. For example, the presence of longitudinal gauge bosons from heavy Higgs decays have been studied in earlier works in the context of Tevatron [63]. LHC analyses have also looked at features of longitudinal gauge bosons in the SM [64].



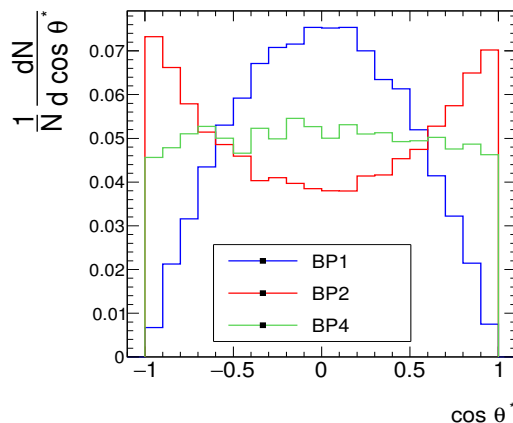


**Figure 3.** Normalized distribution of  $\cos \theta^*$  of the negatively charged lepton ( $\ell^-$ ) arising from the  $\tilde{\chi}_1^0$  NLSP decay at rest corresponding to the benchmarks **BP1**, **BP2** and **BP4** with the isolation variable  $\Delta R > 0.2$  for the leptons.

In case an excess over SM is observed, it is of crucial importance to extend current search strategies to characterize BSM scenarios by studying variables sensitive to the polarisation information of the gauge bosons via their decay products. Although there have been several studies in the context of  $e^+e^-$  colliders focusing on studies of polarisations of the incoming electron-positron beams or polarisation of the final state particles, there are few analogous studies with respect to the LHC utilising these techniques [65]. The polarisation of a  $Z$  boson has been studied briefly in [65] with respect to the LHC in a similar scenario however in displaced dilepton final states arising from the  $Z$  boson decay using the angular variable  $\cos \theta^*$  discussed below. We discuss analytically some basic variables found in the literature, which distinguish longitudinal and transverse gauge bosons. The differential decay rates for the transversely polarized and longitudinally polarized  $Z$  boson in the rest frame of  $Z$  boson are [63]:

$$\frac{d\Gamma_T}{d\cos \theta^*} \propto (1 \pm \cos \theta^*)^2 \quad (7.7.1)$$

$$\frac{d\Gamma_L}{d\cos \theta^*} \propto \sin^2 \theta^* \quad (7.7.2)$$

where  $\Gamma_T = \Gamma(\tilde{\chi}_1^0 \rightarrow Z_T \tilde{G})$  and  $\Gamma_L = \Gamma(\tilde{\chi}_1^0 \rightarrow Z_L \tilde{G})$  are the partial decay widths of the  $\tilde{\chi}_1^0$  to a transverse  $Z$  boson ( $Z_T$ ) and longitudinal  $Z$  ( $Z_L$ ) boson respectively. The angle  $\theta^*$  is defined as the angle the outgoing lepton (arising from the  $Z$  boson decay) makes with the  $Z$  boson in its rest frame with the reference direction being the boost direction of the  $Z$  boson in the laboratory frame. The dependence of the decay width, *i.e.*  $(1 \pm \cos \theta^*)^2$  corresponds to  $k = \mp 1$  state and  $\sin^2 \theta^*$  corresponds



to  $k = 0$  state, where  $k$  is the helicity of the  $Z$  boson. To highlight the difference we choose the NLSP from a few of the benchmarks we had chosen for our analysis and generate a normalized distribution for  $\cos \theta^*$  where the NLSP is decaying at rest and gives the  $Z$  boson as its decay product. The simple illustration of this reconstruction is shown in Figure 3 where **BP1** represents a dominantly higgsino-like NLSP, **BP2** represents a dominantly gaugino-like NLSP while **BP4** represents a somewhat democratic admixture of higgsinos and gauginos in the NLSP.

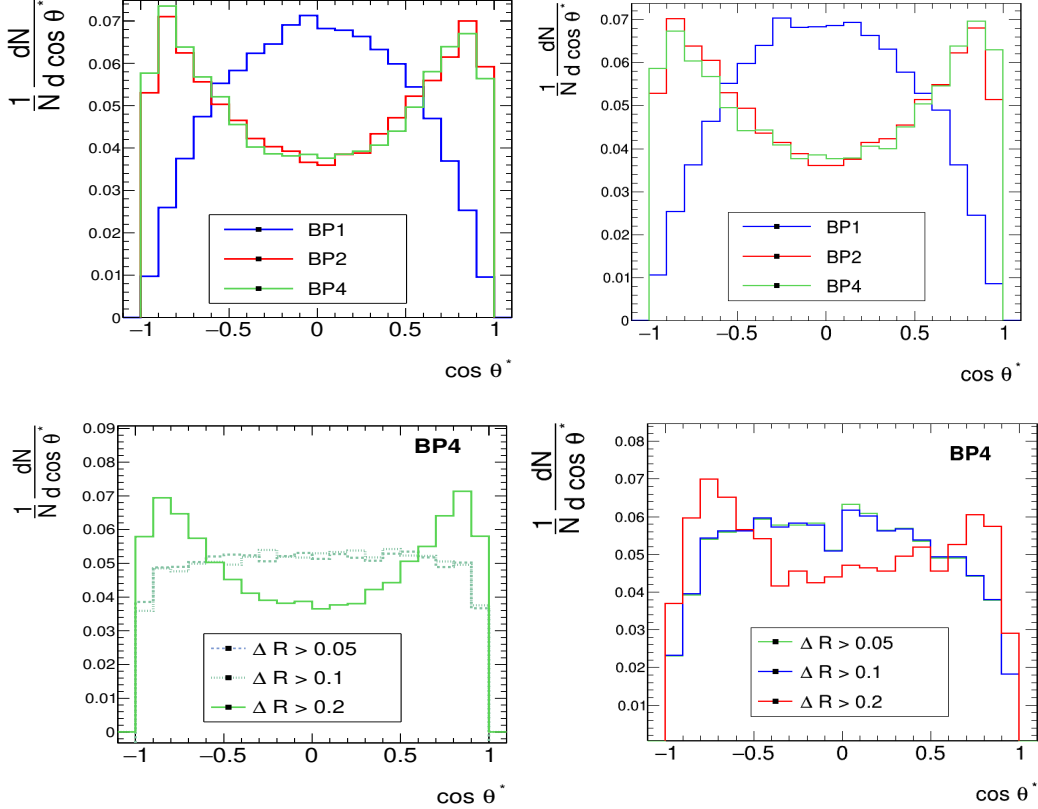


**Figure 4.** Normalized distribution of  $\cos \theta^*$  of the negatively charged lepton ( $\ell^-$ ) arising from the  $\tilde{\chi}_1^0$  NLSP at the parton level (top left panel) and after detector simulation (top right panel) using **Analysis 1**, corresponding to the benchmarks **BP1**, **BP2** and **BP4**. In the bottom panel we present the plots for **BP4** at the parton level (left) and at the detector level (right) for various  $\Delta R$  values as discussed in the text.

We now go ahead and consider the full analysis for the signal  $\geq 1 b + \ell^+ \ell^- + \cancel{E}_T$  and focus on the negatively charged lepton. Note that we expect the nature of the NLSP as highlighted in Figure 3 for the  $Z$  polarisation to be robust against the energy smearings in the detector and the full detector simulation. To show this we compare both parton-level analysis to the signal events obtained after detector simulations. We plot the normalized distributions for  $\cos \theta^*$  of the negatively charged daughter lepton of the  $Z$  boson in Figure 4 at the parton level (left) and detector level

(right-panel) for our benchmarks **BP1**, **BP2** and **BP4** where one NLSP decays to a  $Z$  boson along with a  $\tilde{G}$ . Recall, **BP1** a purely higgsino-like NLSP ( $\sim 99\%$ ), **BP2** purely gaugino-like NLSP ( $\sim 100\%$ ) and **BP4** has  $\sim 31\%$  gaugino admixture in the NLSP. Note that charge identification of the lepton ( $\ell^-$ ) is important in determining the polarisation information of the parent  $Z$  boson. We observe in Figure 4 that the distributions for the negatively charged lepton (for **BP1** and **BP2**) bear significant resemblance at both parton and detector level simulations, to the expected distributions as shown in Figure 3 and follows Eq. 7.7.1 and Eq. 7.7.2 for the longitudinally polarised  $Z$  boson ( $\cos \theta^* = 0$ ) and the transversely polarised  $Z$  boson ( $\cos \theta^* = \pm 1$ ). For **BP4** where the NLSP is a more democratic superposition of the higgsino and gaugino states, owing to the presence of a considerable fraction of gaugino admixture in the NLSP gives rise to a slightly flat and broad peak for  $\cos \theta^*$  in Figure 3. In addition, the NLSP mass is around 2 TeV which results in a very boosted  $Z$  boson in the final state. The event selection criteria can in principle have adverse effects in this case and modify the distributions. The most notable effect for **BP4** that we find is that the distribution starts to resemble features similar to the gaugino-like NLSP (**BP2**) at both parton and detector-level simulations. This we find is due to the fact that when the  $Z$  boson is highly boosted, the pair of charged leptons coming from the  $Z$  boson decay get more collimated with a very small opening angle. This in turn would mean that a larger isolation requirement for the charged leptons would lead to loss of events and also affect the  $\cos \theta^*$  distribution. Note that in our analysis we have used the default Delphes card using a small cone radius  $R = 0.2$  and a maximum energy deposit in the cone being 10% of the  $p_T$  of the lepton as used for electron identification. An isolation cut on  $\Delta R > 0.2$  when used seems to reduce the peak of the  $\cos \theta^*$  plot due to the leptons getting rejected under the isolation cut. To counter this, for **BP4** we find that a much loose lepton identification criterion can be useful for our purpose. To highlight this we identify the charged leptons with a much larger cone radius of  $R = 0.5$  for lepton identification and also demand that a large energy deposit with respect to the  $p_T$  of the lepton is allowed in the cone ( $\sim 12\%$  for electrons and  $25\%$  for muons). The distribution still retains the gaugino-like behaviour for an isolation of  $\Delta R > 0.2$  as in the parton level but starts agreeing with the higgsino-like feature (as in the parton-level case) when the separation between the charged leptons is chosen to be loose with  $\Delta R > 0.05$  or  $\Delta R > 0.1$  as can be seen in the bottom-right panel of Figure 4.

The qualitative differences observed in the distributions of the negatively charged lepton as the gaugino admixture increases in the NLSP amongst the three cases may be effectively captured by defining asymmetry variables in  $\cos \theta^*$  which could clearly discriminate between a dominantly longitudinal and dominantly transverse  $Z$  boson. Taking a cue from the features of  $\cos \theta^*$ , we construct a variable which enhances this difference through an asymmetry amongst the observed  $\cos \theta^*$  values for the higgsino-like and gaugino-like NLSP. The asymmetry variable,  $C_{\theta_Z}$ , as defined

Benchmark	$m_{\tilde{\chi}_1^0}$ (GeV)	Higgsino admixture (%)	Gaugino admixture (%)	$C_{\theta_Z}^{\text{rest}}$	$C_{\theta_Z}^{\text{parton}}$	$C_{\theta_Z}$	$C_Z$
<b>BP1</b>	810.9	99.83	0.17	0.378	0.332	0.346	0.377
	1606.4	99.35	0.65	0.368	0.268	0.286	0.279
	1995.8	97.58	2.42	0.19	0.120	0.198	0.169
<b>BP4</b>	2211.0	68.31	31.69	0.021	-0.309	-0.214	-0.209
<b>BP2</b>	797.9	0.05	99.95	-0.18	-0.078	-0.054	-0.025

**Table 8.** Variation of the asymmetry variables  $C_{\theta_Z}^{\text{rest}}$ ,  $C_{\theta_Z}^{\text{parton}}$ ,  $C_{\theta_Z}$  and  $C_Z$  as defined in the text, at the parton-level and detector level after cuts **D1-D5** for benchmarks **BP1**, **BP2**, **BP4** and some intermediate points with different gaugino-higgsino admixture.

in Equation 7.7.3, serves to enhance the features of the longitudinally polarised  $Z$  boson in comparison to the transversely polarised  $Z$  boson such that they would be less affected if detector simulation effects smear the polarisation dependence of the angular or energy observables. We define

$$C_{\theta_Z} = \frac{N_A - N_B - N_C}{N_A + N_B + N_C} \quad (7.7.3)$$

where  $N_I$ 's stand for events whereas the subscript  $I = A, B, C$  represent the angular regions in  $\theta^*$  given by  $A = [\pi/3, 2\pi/3]$ ,  $B = [0, \pi/3]$  and  $C = [2\pi/3, \pi]$ . The numerator focuses only on the asymmetry features while the denominator is the total number of events for  $-1 < \cos \theta^* < 1$ . Based on the construction of  $C_{\theta_Z}$  a positive value is indicative of a higgsino-like NLSP whereas negative values indicate a gaugino-like NLSP. Since  $C_{\theta_Z}$  is the normalised difference in the number of events corresponding to  $|\cos \theta^*| < 0.5$  and  $|\cos \theta^*| > 0.5$ , a higgsino-like NLSP which gives larger events around  $\cos \theta^* = 0$   $N_A > (N_B + N_C)$  whereas for the gaugino-like NLSP the distribution peaks around  $\cos \theta^* \sim \pm 0.8$  i.e.  $(N_B + N_C) > N_A$ . Therefore the latter shows a negative sign as compared to the former. We enlist the values of  $C_{\theta_Z}$  for cases when the NLSP decays at rest ( $C_{\theta_Z}^{\text{rest}}$ ) and compare this with parton-level ( $C_{\theta_Z}^{\text{parton}}$ ) results and full detector-level simulation ( $C_{\theta_Z}$ ) of our **Analysis 1** in Table 8 for the benchmarks **BP1**, **BP2** and **BP4**. We also include results for a few intermediate points with varying NLSP mass and compositions, after the selection cuts **D1-D5** are applied.<sup>6</sup>

Note that the values of  $C_{\theta_Z}$  are in good agreement with the parton level  $C_{\theta_Z}^{\text{parton}}$  results, from squark pair production. They also agree to almost all results from the NLSP decaying at rest as discussed in Figure 3 with slight variations arising due to isolation cuts and smearing effects at the detector level, except for **BP4**. At

<sup>6</sup>The results in Table 8 are produced by using only squark pair production. However the generic feature remains unchanged even when all production modes are included.

the parton level,  $C_{\theta_Z}^{\text{parton}}$  values range from  $[-0.08 : 0.33]$  as one varies the gaugino-higgsino admixture in the NLSP. For the pure higgsino-like NLSP (**BP1**),  $C_{\theta_Z}$  is large and positive owing to the large higgsino-fraction in the NLSP whereas the pure gaugino-like NLSP **BP2** shows a negative value. For **BP1**,  $C_{\theta_Z}$  is large and positive with the value decreasing as the gaugino admixture starts increasing. We illustrate this variation upon choosing a similar benchmark as **BP1** differing in the choice of  $\mu$  ranging from 1.6 - 1.8 TeV to illustrate this effect. As one considers a dominantly gaugino-like NLSP as in **BP2**,  $C_{\theta_Z}$  turns negative. Thus, with increasing gaugino admixture, the asymmetry value is negative and may be used as an estimate to determine the composition of the NLSP. The detector level estimates for  $C_{\theta_Z}$  are similar to their parton level estimates. The most notable change is observed for the **BP4** with an intermediate gaugino-higgsino admixture.  $C_{\theta_Z}$  value is  $\sim 0.021$  when the NLSP decays at rest with the small positive value still hinting at a larger higgsino admixture. However it turns negative for the analysis where the NLSP appears from cascade decays of the squark, both at the parton and the detector level owing largely to the effect of isolation cuts and detector smearing effects which modify the  $\cos \theta^*$  distribution as seen in Fig 4 and discussed earlier. We note that the  $C_{\theta_Z}^{\text{parton}}$  value becomes positive giving  $C_{\theta_Z}^{\text{parton}} = 0.04, 0.05$  for the loose isolation requirement and identification of the charged lepton with  $\Delta R > 0.05, 0.1$  as expected from Figure 4 as against  $C_{\theta_Z}^{\text{parton}} = -0.214$  for the tighter isolation cut of  $\Delta R > 0.2$ . We expect that the same would be true when the events are passed through detector simulations which would be consistent with observations made in the lower panels of Figure 4.

It is worth pointing out here that **BP4** has a very heavy higgsino NLSP, and the equivalence theorem [62] suggests that the couplings of the longitudinal mode are enhanced as the mass of the NLSP increases (which ensures a large fraction of the longitudinal polarisation mode in the  $Z$  boson), the asymmetry variable is expected to capture this effect as one increases the mass of the NLSP. However, as the mass splitting becomes too large the  $Z$  boson gets more boosted which makes the opening angle between the charged lepton pair very small leading to reduction of isolated dilepton events. Thus the asymmetry values in Table 8 for the heavier NLSP values are unable to reflect this feature.

An additional kinematic feature that can be used to study the polarisation of the  $Z$  boson which in effect highlights the composition of the NLSP is the charged lepton energy. Among others, the ratio of the energy carried by the charged lepton and antilepton also show a dependence on the polarisation of the  $Z$  boson with an energy  $E$ , via dependence on the angle  $\theta^*$ . The energy ( $E_\ell$ ) of the leptons emitted at an angle  $\theta^*$  with respect to the boost direction  $\beta$  of the  $Z$  boson in the laboratory frame [63] follows:

$$E_\ell \propto \frac{E}{2}(1 \pm \beta \cos \theta^*) \quad (7.7.4)$$

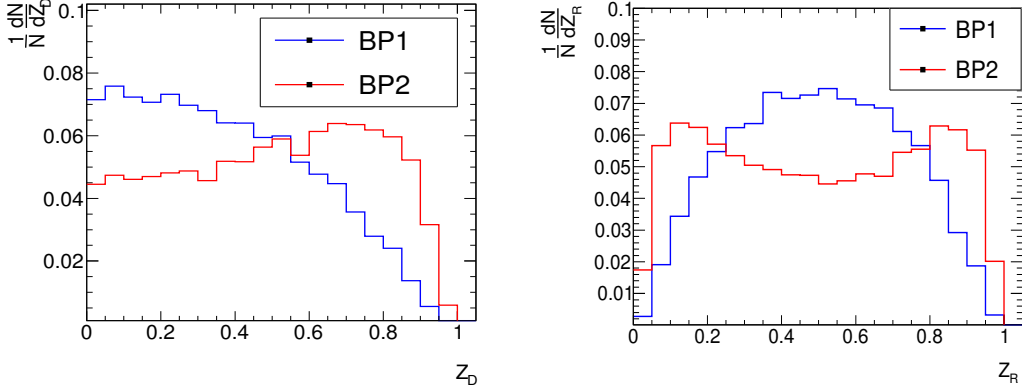


**Figure 5.** Normalized distributions of the kinematic variables  $Z_D$  and  $Z_R$  as defined in the text for distinguishing between a higgsino and gaugino-like  $\tilde{\chi}_1^0$  NLSP before cuts **D1-D5**. The variables are as defined in the text. Here, we have plotted the observables for the process  $\tilde{q}\tilde{q}$  with one of the squarks decaying as:  $\tilde{q} \rightarrow q\tilde{\chi}_1^0 \rightarrow qZ\tilde{G}, Z \rightarrow \ell^+\ell^-$ .

Using this we define two kinematic variables  $Z_D$  and  $Z_R$  (variations of such variables have been pointed out in earlier papers [66, 67] using jet substructure to study hadronic final states) :

$$Z_D = (E_{\ell^-} - E_{\ell^+})/(E_{\ell^-} + E_{\ell^+}); \quad Z_R = E_{\ell^-}/(E_{\ell^-} + E_{\ell^+}) \quad (7.7.5)$$

We study the feasibility of these variables using simple cuts on kinematic variables and ascertain their efficacy after detector simulation effects are taken into account. Note that the energies of the leptons from  $Z$  decay also carry the information of the polarisation of the parent. For a predominantly longitudinal  $Z$  boson, there is an equal sharing of energy of the parent among its daughter particles whereas for a transverse  $Z$  boson, the energy sharing is unequal. The asymmetry is evident in Fig 5 where the higgsino-like NLSP peaks at  $Z_D = 0.1$  as compared to  $Z_D = 0.8$  for the gaugino-like case. Similar effects are observed in the variable  $Z_R$  which denotes the fraction of net leptonic energy carried away by the negatively charged lepton. The ratio peaks at  $Z_R \simeq 0.5$  for **BP1** as compared to  $Z_R \simeq 0.1$  and  $Z_R \simeq 0.8$  for the **BP2** since for the former case, the leptons mostly have equal energy sharing whereas unequal energy sharing occurs for the latter case. We define an asymmetry variable similar to  $C_{\theta_Z}$ , now referred to as  $C_Z$  to capture the asymmetry in the values of  $Z_D$  at the detector level.

$$C_Z = \frac{N_B - N_A}{N_A + N_B} \quad (7.7.6)$$

where  $N_A$  refers to the number of events for  $Z_D < 0.5$  and  $N_B$  represents events for  $Z_D > 0.5$  respectively. We enlist the  $C_Z$  values in Table 8 and observe that  $C_Z$  is positive for the higgsino-like NLSP and negative for gaugino-like NLSP. Note

that the effect observed for the highly boosted  $Z$  boson in  $C_{\theta_Z}$  also shows up for  $C_Z$  highlighting the consistency and importance of the isolation of the charged leptons.

Therefore we emphasise that the distribution of  $\cos \theta^*$  using charge identification of the leptons arising from the  $Z$  boson decay as well as the associated asymmetry variables,  $C_{\theta_Z}$  and  $C_Z$  prove quite efficient in identifying the nature of the NLSP. The distinctive features of the variables discussed for distinguishing a longitudinal and transversely polarised  $Z$  boson are also applicable for new physics scenarios where a polarised gauge boson is likely to be produced, and therefore can prove very important in studying BSM physics.

## 8 Summary and Conclusions

In this work, we have considered higgsino-like  $\tilde{\chi}_1^0$  NLSP in the presence of a light keV  $\tilde{G}$  LSP in the framework of phenomenological MSSM. The keV scale  $\tilde{G}$  serves as a warm dark matter candidate, significantly relaxing constraints from dark matter searches on the MSSM spectra and thereby allowing low  $\mu$  parameter values. In addition, presence of a light  $\tilde{G}$  allows decay of  $\tilde{\chi}_1^0$  NLSP to a Higgs/ $Z$  boson and  $\tilde{G}$  leading to hard  $b$ -jets and charged leptons in the final state along with large  $\cancel{E}_T$  carried away by the  $\tilde{G}$ . Such a scenario has been extensively explored by experiments, including the LHC with primary focus on the low-lying electroweak sector, leading to stringent constraints on the parameter space. The question that one ventures to answer in this study is as follows: *What are the future prospects of detecting a higgsino-like  $\tilde{\chi}_1^0$  NLSP at LHC? If detected, how can we ascertain the nature of the NLSP?*

We address this question by studying a specific final state:  $\geq 1b + \ell^+\ell^- + \cancel{E}_T$  at  $\sqrt{s} = 13$  TeV motivated by the presence of atleast a couple of  $b$ -jets from the Higgs and an opposite-sign same flavour lepton pair from  $Z$  boson decay besides large  $\cancel{E}_T$ . We choose a few representative benchmark points encompassing a light and heavy higgsino sector with/without strong sector sparticles within the reach of LHC. We find that such a signal is discoverable in the upcoming runs of the high luminosity LHC after suitable cuts are applied. It is important to emphasise that such a semi-leptonic channel will prove crucial in identifying the nature of the NLSP, being relatively clean compared to an all hadronic final state which may have a better discovery prospect. Thus simultaneous use of both channels could be advocated for the purpose of discovery and identifying the nature of the NLSP. We focus on the presence of a dominantly longitudinal  $Z$  boson arising from the decay of a higgsino-like  $\tilde{\chi}_1^0$  owing to the presence of the Goldstone boson as the longitudinal mode of  $Z$  after electroweak symmetry breaking. This is quite a striking identification criteria if observable for a higgsino-like NLSP in sharp contrast to a dominantly gaugino-like NLSP, which would dominantly decay to a transversely polarised  $Z$ . It is thus important to characterise the features of the longitudinally polarised  $Z$  boson to

ascertain the composition of the parent  $\tilde{\chi}_1^0$ . The effects of polarisation of the  $Z$  boson is carried by its decay products, namely, the leptons through their angular distributions. We construct several kinematic variables using the negatively charged lepton as reference and highlight its importance in observing the polarisation of the parent gauge boson. We also propose new variables which utilise the observed asymmetries between the angular variables for the charged lepton coming from a parent longitudinal and transverse  $Z$  boson. We do a full detector level simulation of the events and study the asymmetries that show the characteristic features of a longitudinal  $Z$  boson and observe substantial differences between a higgsino and gaugino-like NLSP, which highlights the robustness of the constructed asymmetries. Our analysis is equally applicable to other BSM scenarios and will prove useful in studying scenarios which project out the longitudinal nature of the weak gauge bosons and in the process highlight the veracity of the equivalence theorem in a relatively nonchalant way.

## Acknowledgements

The work is partially supported by funding available from the Department of Atomic Energy, Government of India, for the Regional Centre for Accelerator-based Particle Physics (RECAPP), Harish-Chandra Research Institute(HRI). The research of JD is also partially supported by the INFOSYS scholarship for senior students at the Harish-Chandra Research Institute. We thank A. Ghosh, P.Konar, S. Mondal and T. Samui for helpful comments, and K. Hagiwara for illuminating discussions.

## References

- [1] **ATLAS** Collaboration, <https://atlas.web.cern.ch/Atlas/GROUPS/PHYSICS/CombinedSummaryPlots/SUSY/>.
- [2] **CMS** Collaboration, <https://twiki.cern.ch/twiki/bin/view/CMSPublic/PhysicsResultsSUS>.
- [3] **Planck** Collaboration, N. Aghanim et al., *Planck 2018 results. VI. Cosmological parameters*, [arXiv:1807.06209](https://arxiv.org/abs/1807.06209).
- [4] M. Ibe, A. Kamada, and S. Matsumoto, *Mixed (cold+warm) dark matter in the bino-wino coannihilation scenario*, *Phys. Rev.* **D89** (2014), no. 12 123506, [[arXiv:1311.2162](https://arxiv.org/abs/1311.2162)].
- [5] G. Arcadi, M. Dutra, P. Ghosh, M. Lindner, Y. Mambrini, M. Pierre, S. Profumo, and F. S. Queiroz, *The waning of the wimp? a review of models, searches, and constraints*, *The European Physical Journal C* **78** (Mar, 2018) 203.
- [6] H. Baer, V. Barger, D. Sengupta, and X. Tata, *Is natural higgsino-only dark matter excluded?*, *Eur. Phys. J.* **C78** (2018), no. 10 838, [[arXiv:1803.11210](https://arxiv.org/abs/1803.11210)].



- [7] M. Abdughani, L. Wu, and J. M. Yang, *Status and prospects of light binohiggsino dark matter in natural SUSY*, *Eur. Phys. J.* **C78** (2018), no. 1 4, [[arXiv:1705.09164](#)].
- [8] S. P. Martin, *A Supersymmetry primer*, [hep-ph/9709356](#). [Adv. Ser. Direct. High Energy Phys.18,1(1998)].
- [9] M. Drees, R. Godbole, and P. Roy, *Theory and phenomenology of sparticles: An account of four-dimensional N=1 supersymmetry in high energy physics*. 2004.
- [10] G. F. Giudice and R. Rattazzi, *Theories with gauge mediated supersymmetry breaking*, *Phys. Rept.* **322** (1999) 419–499, [[hep-ph/9801271](#)].
- [11] J. Baur, N. Palanque-Delabrouille, C. Yche, C. Magneville, and M. Viel, *Lyman-alpha Forests cool Warm Dark Matter*, *JCAP* **1608** (2016), no. 08 012, [[arXiv:1512.01981](#)].
- [12] A. Boyarsky, J. Lesgourgues, O. Ruchayskiy, and M. Viel, *Lyman-alpha constraints on warm and on warm-plus-cold dark matter models*, *Journal of Cosmology and Astroparticle Physics* **2009** (may, 2009) 012–012.
- [13] L. Covi, *DARK MATTER CANDIDATES: AXINO AND GRAVITINO*, in *Proceedings, 46th Rencontres de Moriond on Electroweak Interactions and Unified Theories: La Thuile, Italy, March 13-20, 2011*, pp. 381–388.
- [14] P. Meade, M. Reece, and D. Shih, *Prompt Decays of General Neutralino NLSPs at the Tevatron*, *JHEP* **05** (2010) 105, [[arXiv:0911.4130](#)].
- [15] K. T. Matchev and S. D. Thomas, *Higgs and Z boson signatures of supersymmetry*, *Phys. Rev.* **D62** (2000) 077702, [[hep-ph/9908482](#)].
- [16] **CMS** Collaboration, A. M. Sirunyan et al., *Combined search for electroweak production of charginos and neutralinos in proton-proton collisions at  $\sqrt{s} = 13$  TeV*, *JHEP* **03** (2018) 160, [[arXiv:1801.03957](#)].
- [17] **ATLAS** Collaboration, [https://atlas.web.cern.ch/Atlas/GROUPS/PHYSICS/CombinedSummaryPlots/SUSY/ATLAS\\_SUSY\\_EWSummary\\_GGM/ATLAS\\_SUSY\\_EWSummary\\_GGM.png](https://atlas.web.cern.ch/Atlas/GROUPS/PHYSICS/CombinedSummaryPlots/SUSY/ATLAS_SUSY_EWSummary_GGM/ATLAS_SUSY_EWSummary_GGM.png).
- [18] H. Baer, V. Barger, P. Huang, D. Mickelson, A. Mustafayev, and X. Tata, *Radiative natural supersymmetry: Reconciling electroweak fine-tuning and the Higgs boson mass*, *Phys. Rev.* **D87** (2013), no. 11 115028, [[arXiv:1212.2655](#)].
- [19] H. Baer, V. Barger, P. Huang, D. Mickelson, A. Mustafayev, and X. Tata, *Naturalness, Supersymmetry and Light Higgsinos: A Snowmass Whitepaper*, in *Proceedings, Community Summer Study 2013: Snowmass on the Mississippi (CSS2013): Minneapolis, MN, USA, July 29-August 6, 2013*, 2013. [[arXiv:1306.2926](#)].
- [20] A. Mustafayev and X. Tata, *Supersymmetry, Naturalness, and Light Higgsinos*, *Indian J. Phys.* **88** (2014) 991–1004, [[arXiv:1404.1386](#)].



- [21] H. Baer, V. Barger, P. Huang, A. Mustafayev, and X. Tata, *Radiative natural SUSY with a 125 GeV Higgs boson*, *Phys. Rev. Lett.* **109** (2012) 161802, [[arXiv:1207.3343](#)].
- [22] H. Baer, V. Barger, M. Savoy, and X. Tata, *Multichannel assault on natural supersymmetry at the high luminosity LHC*, *Phys. Rev.* **D94** (2016), no. 3 035025, [[arXiv:1604.07438](#)].
- [23] H. Baer, V. Barger, J. S. Gainer, P. Huang, M. Savoy, D. Sengupta, and X. Tata, *Gluino reach and mass extraction at the LHC in radiatively-driven natural susy*, *The European Physical Journal C* **77** (Jul, 2017) 499.
- [24] H. Baer and X. Tata, *Weak scale supersymmetry: From superfields to scattering events*. Cambridge University Press, 2006.
- [25] **CMS Collaboration** Collaboration, *Search for disappearing tracks in proton-proton collisions at  $\sqrt{s} = 13$  TeV*, Tech. Rep. CMS-PAS-EXO-16-044, CERN, Geneva, 2018.
- [26] **ATLAS Collaboration**, M. Aaboud et al., *Search for metastable heavy charged particles with large ionization energy loss in pp collisions at  $\sqrt{s} = 13$  TeV using the ATLAS experiment*, *Phys. Rev.* **D93** (2016), no. 11 112015, [[arXiv:1604.04520](#)].
- [27] S. Raby, *Long-lived gluinos and stable axinos*, *Phys. Rev. Lett.* **115** (Dec, 2015) 231801.
- [28] L. Covi, J. Hasenkamp, S. Pokorski, and J. Roberts, *Gravitino Dark Matter and general neutralino NLSP*, *JHEP* **11** (2009) 003, [[arXiv:0908.3399](#)].
- [29] M. Drees, M. M. Nojiri, D. P. Roy, and Y. Yamada, *Light Higgsino dark matter*, *Phys. Rev.* **D56** (1997) 276–290, [[hep-ph/9701219](#)]. [Erratum: *Phys. Rev.* **D64**, 039901 (2001)].
- [30] G. F. Giudice and A. Pomarol, *Mass degeneracy of the Higgsinos*, *Phys. Lett.* **B372** (1996) 253–258, [[hep-ph/9512337](#)].
- [31] A. Djouadi, *The Anatomy of electro-weak symmetry breaking. II. The Higgs bosons in the minimal supersymmetric model*, *Phys. Rept.* **459** (2008) 1–241, [[hep-ph/0503173](#)].
- [32] **CMS Collaboration**, A. M. Sirunyan et al., *Combined measurements of Higgs boson couplings in proton-proton collisions at  $\sqrt{s} = 13$  TeV*, Submitted to: *Eur. Phys. J.* (2018) [[arXiv:1809.10733](#)].
- [33] **CMS Collaboration**, S. Chatrchyan et al., *Observation of a new boson at a mass of 125 GeV with the CMS experiment at the LHC*, *Phys. Lett.* **B716** (2012) 30–61, [[arXiv:1207.7235](#)].
- [34] W. Porod, *SPheno, a program for calculating supersymmetric spectra, SUSY particle decays and SUSY particle production at  $e^+ e^-$  colliders*, *Comput. Phys. Commun.* **153** (2003) 275–315, [[hep-ph/0301101](#)].
- [35] W. Porod and F. Staub, *SPheno 3.1: Extensions including flavour, CP-phases and*

- models beyond the MSSM*, *Comput. Phys. Commun.* **183** (2012) 2458–2469, [[arXiv:1104.1573](#)].
- [36] **ATLAS** Collaboration, M. Aaboud et al., *Search for pair production of higgsinos in final states with at least three b-tagged jets in  $\sqrt{s} = 13$  TeV pp collisions using the ATLAS detector*, *Submitted to: Phys. Rev.* (2018) [[arXiv:1806.04030](#)].
  - [37] **CMS** Collaboration, A. M. Sirunyan et al., *Search for Physics Beyond the Standard Model in Events with High-Momentum Higgs Bosons and Missing Transverse Momentum in Proton-Proton Collisions at 13 TeV*, *Phys. Rev. Lett.* **120** (2018), no. 24 241801, [[arXiv:1712.08501](#)].
  - [38] **ATLAS** Collaboration, M. Aaboud et al., *Search for supersymmetry in events with four or more leptons in  $\sqrt{s} = 13$  TeV pp collisions with ATLAS*, [arXiv:1804.03602](#).
  - [39] **ATLAS** Collaboration, M. Aaboud et al., *Search for squarks and gluinos in final states with jets and missing transverse momentum using  $36\text{fb}^{-1}$  of  $\sqrt{s} = 13\text{TeV}$  pp collision data with the ATLAS detector*, *Phys. Rev.* **D97** (2018), no. 11 112001, [[arXiv:1712.02332](#)].
  - [40] **ATLAS** Collaboration, M. Aaboud et al., *Search for chargino and neutralino production in final states with a Higgs boson and missing transverse momentum at  $\sqrt{s} = 13$  TeV with the ATLAS detector*, [arXiv:1812.09432](#).
  - [41] **CMS** Collaboration, A. M. Sirunyan et al., *Search for new phenomena in final states with two opposite-charge, same-flavor leptons, jets, and missing transverse momentum in pp collisions at  $\sqrt{s} = 13$  TeV*, *JHEP* **03** (2018) 076, [[arXiv:1709.08908](#)].
  - [42] **CMS Collaboration** Collaboration, *Search for physics beyond the standard model in events with high-momentum higgs bosons and missing transverse momentum in proton-proton collisions at 13 tev*, *Phys. Rev. Lett.* **120** (Jun, 2018) 241801.
  - [43] J. Dutta, P. Konar, S. Mondal, B. Mukhopadhyaya, and S. K. Rai, *Search for a compressed supersymmetric spectrum with a light Gravitino*, *JHEP* **09** (2017) 026, [[arXiv:1704.04617](#)].
  - [44] A. Arbey, M. Battaglia, A. Djouadi, F. Mahmoudi, and J. Quevillon, *Implications of a 125 gev higgs for supersymmetric models*, *Physics Letters B* **708** (2012), no. 1 162 – 169.
  - [45] LEPSUSYWG et al., *Lep2 susy working group*, .  
<http://lepsusy.web.cern.ch/lepsusy/>.
  - [46] M. Drees, H. Dreiner, D. Schmeier, J. Tattersall, and J. S. Kim, *CheckMATE: Confronting your Favourite New Physics Model with LHC Data*, *Comput. Phys. Commun.* **187** (2015) 227–265, [[arXiv:1312.2591](#)].
  - [47] J. Alwall, R. Frederix, S. Frixione, V. Hirschi, F. Maltoni, O. Mattelaer, H. S. Shao, T. Stelzer, P. Torrielli, and M. Zaro, *The automated computation of tree-level and*

- next-to-leading order differential cross sections, and their matching to parton shower simulations, *JHEP* **07** (2014) 079, [[arXiv:1405.0301](#)].
- [48] N. D. Christensen, P. de Aquino, N. Deutschmann, C. Duhr, B. Fuks, C. Garcia-Cely, O. Mattelaer, K. Mawatari, B. Oexl, and Y. Takaesu, *Simulating spin-3/2 particles at colliders*, *The European Physical Journal C* **73** (Oct, 2013) 2580.
  - [49] T. Sjostrand, S. Mrenna, and P. Z. Skands, *PYTHIA 6.4 Physics and Manual*, *JHEP* **05** (2006) 026, [[hep-ph/0603175](#)].
  - [50] Pythia. <http://home.thep.lu.se/~torbjorn/pythia81html/Welcome.html>.
  - [51] **DELPHES 3** Collaboration, J. de Favereau, C. Delaere, P. Demin, A. Giammanco, V. Lematre, A. Mertens, and M. Selvaggi, *DELPHES 3, A modular framework for fast simulation of a generic collider experiment*, *JHEP* **02** (2014) 057, [[arXiv:1307.6346](#)].
  - [52] M. Cacciari, G. P. Salam, and G. Soyez, *The Anti- $k(t)$  jet clustering algorithm*, *JHEP* **04** (2008) 063, [[arXiv:0802.1189](#)].
  - [53] M. Cacciari, G. P. Salam, and G. Soyez, *FastJet User Manual*, *Eur. Phys. J.* **C72** (2012) 1896, [[arXiv:1111.6097](#)].
  - [54] H.-C. Cheng and Z. Han, *Minimal Kinematic Constraints and  $m(T2)$* , *JHEP* **12** (2008) 063, [[arXiv:0810.5178](#)].
  - [55] W. Beenakker, R. Hopker, and M. Spira, *PROSPINO: A Program for the production of supersymmetric particles in next-to-leading order QCD*, [hep-ph/9611232](#).  
<http://www.thphys.uni-heidelberg.de/~plehn/index.php?show=prospino&visible=tools>.
  - [56] W. Beenakker, C. Borschensky, M. Krmer, A. Kulesza, E. Laenen, S. Marzani, and J. Rojo, *NLO+NLL squark and gluino production cross-sections with threshold-improved parton distributions*, *Eur. Phys. J.* **C76** (2016), no. 2 53, [[arXiv:1510.00375](#)].
  - [57] L. H. V. cross-sections Working Group.  
<https://twiki.cern.ch/twiki/bin/view/LHCPhysics/LHCHXSWG1HELHCXsecs>.
  - [58] M. Grazzini, S. Kallweit, D. Rathlev, and M. Wiesemann,  *$W^\pm Z$  production at hadron colliders in NNLO QCD*, *Phys. Lett.* **B761** (2016) 179–183, [[arXiv:1604.08576](#)].
  - [59] F. Cascioli, T. Gehrmann, M. Grazzini, S. Kallweit, P. Maierhofer, A. von Manteuffel, S. Pozzorini, D. Rathlev, L. Tancredi, and E. Weihs,  *$ZZ$  production at hadron colliders in NNLO QCD*, *Phys. Lett.* **B735** (2014) 311–313, [[arXiv:1405.2219](#)].
  - [60] M. Czakon, P. Fiedler, and A. Mitov, *Total Top-Quark Pair-Production Cross Section at Hadron Colliders Through  $O(\frac{4}{s})$* , *Phys. Rev. Lett.* **110** (2013) 252004, [[arXiv:1303.6254](#)].
  - [61] L. T. NNLO. [https://twiki.cern.ch/twiki/bin/view/LHCPhysics/TtbarNNLO#Top\\_quark\\_pair\\_cross\\_sections\\_at](https://twiki.cern.ch/twiki/bin/view/LHCPhysics/TtbarNNLO#Top_quark_pair_cross_sections_at).

- [62] V. D. Barjer and R. J.N.Philips, *Collider Physics*. 1991.
- [63] M. Duncan, G. Kane, and W. Repko, *Ww physics at future colliders*, *Nuclear Physics B* **272** (1986), no. 3 517 – 559.
- [64] **ATLAS** Collaboration, M. Aaboud et al., *Measurement of  $W^\pm Z$  production cross sections and gauge boson polarisation in  $pp$  collisions at  $\sqrt{s} = 13$  TeV with the ATLAS detector*, [arXiv:1902.05759](#).
- [65] P. Meade, M. Reece, and D. Shih, *Long-Lived Neutralino NLSPs*, *JHEP* **10** (2010) 067, [[arXiv:1006.4575](#)].
- [66] G. Brooijmans et al., *Les Houches 2017: Physics at TeV Colliders New Physics Working Group Report*, in *10th Les Houches Workshop on Physics at TeV Colliders (PhysTeV 2017) Les Houches, France, June 5-23, 2017*, 2018. [arXiv:1803.10379](#).
- [67] J. R. Andersen et al., *Les Houches 2017: Physics at TeV Colliders Standard Model Working Group Report*, in *10th Les Houches Workshop on Physics at TeV Colliders (PhysTeV 2017) Les Houches, France, June 5-23, 2017*, 2018. [arXiv:1803.07977](#).